

LIBRARY
CALIFORNIA AIR RESOURCES BOARD
P.O. BOX 2815
SACRAMENTO, CA 95812

ACIDIC AEROSOL SIZE DISTRIBUTIONS DURING SCAQS

FINAL REPORT

Prepared for the California Air Resources Board

Contract No. A6-112-32

November 1989

Walter John, Stephen M. Wall, Joseph L. Ondo and Wolfgang Winklmayr

Air and Industrial Hygiene Laboratory

California Department of Health Services

Berkeley, Ca 94704-9980, U.S.A.

The statements and conclusions in this report are those of the contractor and not necessarily those of the California Air Resources Board. The mention of commercial products, their source or their use in connection with the material reported herein is not to be construed as either an actual or implied endorsement of such products.

CONTENTS

Abstract

Introduction

Experimental

Data Analysis

Results

•
Particle Size Distributions

Aerosol Composition and Concentration

Discussion of the Fine Particle Modes

Conclusions

Recommendations

Acknowledgements

References

TABLES

1. Comparison of average mode parameters for nitrate size distributions, Claremont, summer SCAQS, obtained by the data inversion programs of Winklmayr et al. (1988) and Dzubay and Hasan (1989).
2. Average mode parameters for the summer and fall SCAQS periods obtained by fitting the summer mass distributions of the ionic species. Means and standard deviations are listed.
3. Mean concentrations by mode in $\text{neq/m}^3 \pm \text{std. dev.}$

FIGURES

1. Locations of sampling sites.
2. Diagram of sampling assembly.
3. Example of impactor data analysis: (a) stage concentrations, (b) inverted size distribution, (c) solid line, distribution obtained by fitting a sum of lognormal functions to the inverted distribution; dashed lines, the lognormal functions.
4. Examples of nitrate size distributions from Claremont during summer SCAQS. The data were processed as in Figure 3(c).
5. Sulfate size distributions from Long Beach during summer SCAQS.
6. Sulfate size distributions from Rubidoux during summer SCAQS.
7. Ammonium size distributions from Claremont during summer SCAQS.
8. Mode concentrations vs. mode diameter for all sampling sites and all sampling periods during summer SCAQS: Left column, absolute mode concentrations; right column, relative mode concentrations.
9. Relative mode concentration of nitrate vs. mode diameter for all sampling periods during summer SCAQS, from (a) Long Beach, (b) Claremont and (c) Rubidoux.

10. Mode concentrations vs. mode diameter for all sampling sites and all sampling periods during fall SCAQS: Left column, absolute mode concentrations; right column, relative mode concentrations.
11. From all sites during summer SCAQS: Left column, frequency of sulfate, ammonium and nitrate modes vs. mode diameter; right column, average sulfate, nitrate and ammonium concentration vs. mode diameter.
12. From all sites during summer SCAQS: Left column, frequency of sodium, chloride and total ionic mass vs. mode diameter; right column, average sodium, chloride and total ionic mass concentration vs. mode diameter.
13. From all sites during fall SCAQS: Left column, frequency of sulfate, ammonium and nitrate modes vs. mode diameter; right column, average sulfate, ammonium and nitrate mode concentration vs. mode diameter.
14. Ion balance plots for Claremont data during summer SCAQS for the particle size range of the (a) condensation mode, (b) droplet mode, (c) coarse mode and (d) sum of all three modes.
15. Time series of nitrate concentrations during summer SCAQS for the particle size range of the (a) condensation mode, (b) droplet mode and (c) coarse mode.

16. Time series of sulfate concentrations during summer SCAQS for the particle size range of the (a) condensation mode, (b) droplet mode and (c) coarse mode.
17. Time series of nitrate concentrations during fall SCAQS for the particle size range of the (a) condensation mode, (b) droplet mode and (c) coarse mode.
18. Time series of sulfate concentrations during fall SCAQS for the particle size range of the (a) condensation mode, (b) droplet mode and (c) coarse mode.
19. Log-log plot of sulfate mode concentration vs. mode diameter from Claremont during summer SCAQS. The solid lines have slopes corresponding to mode concentration increasing with the cube of the mode diameter. A transition between the two modes is believed to occur at approximately the sulfate mode concentration indicated by the horizontal dashed line.
20. Plot similar to Figure 19 for a sequence of sampling periods at Claremont. Points 1 - 7 are, in order, September 2, periods 1 - 4; September 3, periods 1 - 3.

ABSTRACT

Ambient aerosol in the size range 0.075 - 16 μm was sampled with Berner cascade impactors during the summer and fall intensive sampling periods of the Southern California Air Quality Study (SCAQS) of 1987. Deposits on the greased Tedlar stage substrates were extracted with deionized water and analyzed for inorganic anions and cations by ion chromatography. Stage mass data were inverted by a modified version of the Twomey nonlinear iterative algorithm and modes in the inverted size distributions were fitted with lognormal functions. Nine hundred size distributions of ionic species were obtained.

Three modes, two submicron and one coarse, were sufficient to fit all of the size distributions. The smallest mode, at $0.2 \pm 0.1 \mu\text{m}$ aerodynamic diameter, is probably a condensation mode containing gas phase reaction products. A larger mode, at $0.7 \pm 0.2 \mu\text{m}$, is identified as a droplet mode formed by liquid phase reactions. Evidence was obtained that the droplet mode grew out of the condensation mode by the addition of water and sulfate. During SCAQS, most of the inorganic particle mass was in the droplet mode except during a period of exceptionally low relative humidity. Nitrate was internally mixed with sulfate in the droplet mode. Since most of the aerosol fine mass is included in the ions analyzed, the observed condensation and droplet modes characterize the overall size distribution in the 0.1 - 1 μm range, previously described by Whitby as a single accumulation mode.

Key word index: Size distribution, accumulation mode, condensation, droplet, lognormal, impactor, inorganic, ions, sulfate, nitrate.

INTRODUCTION

Inorganic ions are major constituents of atmospheric aerosol (Appel et al., 1980). Inorganic aerosol reduces visibility, contributes to dry acid deposition and presents a respiratory health hazard. To understand and to model the formation, transport and removal of the inorganic aerosol requires detailed information on the particle size distributions. Therefore, the measurement of the inorganic ion size distributions was an essential component of the Southern California Air Quality Study (SCAQS), a large multigroup effort to provide a comprehensive data base to be used to model air quality in the South Coast Air Basin.

The bimodal size distribution of ambient particles, with an accumulation mode in the size range 0.1 - 1 μm and a coarse mode in the $>1 \mu\text{m}$ range, (Whitby, 1978; Whitby and Sverdrup, 1980) is a powerful generalization, but is based on physical particle sizing methods which do not identify chemical compounds. Additionally, the volume distributions are obtained by transforming number distributions, a procedure inherently inaccurate. Some more recently measured size distributions of atmospheric sulfur aerosol differ from the Whitby distributions. Hering and Friedlander (1982) reported that ambient sulfur occurs in two modes, with mass median aerodynamic diameters of 0.2 μm and 0.5 μm . Their calculations indicated that the smaller mode could be attributed to homogeneous gas phase oxidation of SO_2 and the larger, more common mode to the reaction of SO_2 with preexisting aerosol droplets in the accumulation mode. Wall, et al. (1988) observed both of these modes, sometimes simultaneously, in sulfate measured with a cascade impactor. McMurry and Wilson (1983) reported

observations of sulfur particles as large as 3 μm and accounted for their formation in terms of growth in a droplet phase.

Our group has developed a sampling and data analysis technique capable of resolving multiple modes in the size distributions of ambient inorganic ions. The sampler, a nine-stage Berner cascade impactor, has been carefully calibrated with monodisperse aerosol (Wang and John, 1988). It was found that volatilization losses of ammonium nitrate in the impactor were less than 7% under hot, dry conditions (35^o C, 18% RH) and that ammonium sulfate particles do not grow by water condensation in the expanding jets. A fluorocarbon grease coating on the impactor substrates was shown to prevent particle bounce effectively and not to interfere with ion chemistry. The technique was field-tested at Claremont, CA during the Nitrogen Species Methods Comparison Study (Wall et al., 1988). A nitric acid denuder was placed upstream of the impactor which was run in parallel with a Dichotomous sampler (John et al., 1988). The fine and coarse fractions from the Dichotomous sampler were compared to the corresponding integrated fractions from the impactor. Concentrations of the major ions agreed within about 10% or less. Agreement of the coarse fractions showed that particle loss in the vertical channel of the denuder was not significant. The impactor sampled 8% less fine nitrate than did the Dichotomous sampler, which was equipped with a Nylon afterfilter to recapture any nitrate volatilized from the Teflon prefilter. This was consistent with our laboratory tests. Finally, semi-continuous particle size distributions were obtained from the stage mass data by applying a modified version of the Twomey inversion algorithm.

The measurement technique described above, with improvements which will be discussed, was applied to sampling during SCAQS. This afforded the opportunity

to acquire an extensive data set to investigate the modes in the inorganic ion size distributions and to use the large SCAQS auxiliary data base in the interpretation of the modal structure.

EXPERIMENTAL

Sampling was conducted during the SCAQS intensive study periods, 11 days during the summer from June 19 to September 3, 1987 and 6 days during the fall from November 11 to December 11, 1987. Each study period included a number of 1 - 3 day sampling periods. Sampling began at 0600 the first day of each period and included three 3.5 hr. daytime periods separated by 30 min. changing intervals and one 11.5 hr. overnight period except for the last day of the sampling period which ended at 0100. During the summer, sampling sites included Long Beach near the Pacific coast, Claremont inland and Rubidoux near the eastern end of the basin and downwind of major sources of ammonia. During the fall, the sampling sites were at Long Beach and downtown Los Angeles (See Figure 1).

The sampler is diagrammed in Figure 2. The annular inlet at the top of the nitric acid denuder was located below a rain shield and surrounded by a wind shield. The aluminum denuder was deeply anodized, which gave it a black color. Therefore, it was surrounded by a white PVC sun shield to reduce solar heating effects. An aluminum transition piece provided a smoothly tapered channel from the denuder to the Berner impactor. The sampling train was supported by a stand so that the inlet was at the SCAQS-mandated height of 1.5 m. above the platform which was in turn 0.9 m. above the ground.

In laboratory and field tests (John et al., 1988), we have shown that an anodized aluminum surface absorbs nitric acid efficiently and irreversibly. Laboratory measurements of the efficiencies of the three denuders used at SCAQS yielded an average of $90 \pm 4\%$. The theoretical efficiency was calculated to be 89%, based on the theory of Possanzini et al. (1983) and a diffusion coefficient of $0.118 \text{ cm}^2/\text{s}$ (Durham and Stockburger, 1986). In designing the denuder, we unfortunately used a diffusion coefficient of $0.15 \text{ cm}^2/\text{s}$, which predicted a higher efficiency. Additional removal of nitric acid will occur in the impactor inlet and the first stage, which was used as a precut and not analyzed. Laboratory tests showed that approximately 20% of the nitric acid entering the impactor will be removed before the second stage. The upper ends of the nitrate size particle distributions do not give any indication of nitric acid artifact, which would be maximum on the first analyzed stage and decrease thereafter. Therefore, we believe the protection from nitric acid was adequate.

Three new Berner impactors were acquired for the SCAQS sampling. The critical dimensions were the same as for the prototype we used for the Claremont study, but improvements included all stainless steel parts, a leak-proof gasketing arrangement and an assembly press. Two of the new impactors were run in parallel with the prototype in Berkeley ambient air and the size distributions for inorganic ions compared. Good agreement was obtained between the new impactors and the prototype for supermicron stages, but some discrepancies were evident for submicron stages. Agreement in the ambient size distributions measured by the new impactors and the prototype was achieved by minor adjustments of the cutpoints of the new impactors from the calibrated values obtained for the prototype. This was the basis for the final cutpoints taken for stages 9 through 1 respectively which were 16.5, 8.2, 4.35, 2.15, 1.04, 0.52, 0.27,

0.14 and 0.075 μm . The new adjusted values for stages three and four agree better with theory than did the original calibration values.

The impactor flow rate, nominally 30 L/min, was maintained constant by a critical orifice following the last stage. The exhaust of the rotary carbon vane pump was equipped with a membrane cartridge filter to prevent particle emission. Stage substrates were cut from Tedlar foil in the clean room of a filter manufacturer. Fluorocarbon grease was applied to the foils by solvent evaporation and then the foils were stored in polypropylene extraction tubes. Transfer of the foils to and from the impactors was done in laboratories set up at the sampling sites.

At startup, the pressure downstream of the critical orifice was checked as a precaution against leaks. The flow rate was audited for a brief time by connecting a calibrated rotameter to the inlet. An elapsed time meter was read at the beginning and end of each run. The pressure and flow rate audits were repeated at the end of the run. Static blanks were taken by setting aside foils from each batch. Dynamic blanks were taken by going through the entire normal procedure, but running the pump for only one minute.

After removal from the impactor, the Tedlar foils were returned to the polypropylene tubes, curled with the particle deposit inward. The tube was filled with Argon gas, bagged in plastic and stored on dry ice until just before extraction for analysis in Berkeley. The deposits were extracted in 6 ml of deionized water by placing the tubes horizontally on a rotating "Ferris wheel" for an hour. The solutions were analyzed for anions and cations in a Dionex ion chromatograph with automatic control and data entry into a spreadsheet. The analytical setup included a third channel with a pH microelectrode.

In separate chromatograph runs, a subset of samples were analyzed for divalent calcium and magnesium ions. The subset included samples from stages 6 and 7 only (coarse fraction) which were chosen from 20% of the sampling periods. Each batch of samples included standards and water blanks. We have participated in a number of laboratory intercomparisons for the analysis of inorganic ions which show that the typical accuracy is 3 to 4%. The detection limit (d.l.) is estimated to be 0.25 ug/sample. The average static blanks per sample were 0.5 μg nitrate, < d.l. sulfate and < d.l. ammonium. Average dynamic blanks per sample were 0.3 μg nitrate, 0.3 μg sulfate and < d.l. ammonium. These blank levels are a few percent of the average sample. The uncertainty in the flow rate is about 1%. The overall accuracy in the concentration is estimated to be 5%.

DATA ANALYSIS

The ion stage mass data were inverted by a modified version of the Twomey non-linear iterative algorithm (Winklmayr et al., 1989). This procedure consists of making an initial guess of the particle size distribution and integrating it with the impactor sampling efficiency function to predict the stage masses. These masses are compared to the measured masses, a correction is applied to the size distribution and the process iterated until the stage masses agree within the experimental error. The data inversion improves the size resolution by removing the stage efficiency function and places the results on a more universal basis.

In our initial attempts to invert the data from SCAQS, we encountered difficulties in using the existing versions of the Twomey procedure. We then made

an extensive investigation which resulted in a modified and improved version of the routine. It was found necessary to fit the impactor calibration data with a set of continuous and smooth functions, to use weighting functions for the correction terms, to place constraints on the initial guess distribution, to establish a means of treating zero values and the ends of the distribution and to set iteration stopping criteria based on experimental errors. The routine was tested with numerically created test distributions and SCAQS data.

An example of the data analysis is shown in Figure 3. In (a), a histogram is plotted of the nitrate stage mass concentrations from the morning sampling period at Claremont on July 13, 1987. Figure 3b shows the particle size distribution obtained by inverting the stage data. The semi-continuous distribution consists of 66 particle size intervals. At this step of the procedure the stage efficiency functions have been removed from the data. Then the modes in the inverted distribution are fitted to lognormal functions by least squares. The fitting program begins with the largest mode and adds other modes in decreasing order, stopping when any remaining mode contains less than 5% of the total mass. The size distribution is then characterized by the lognormal parameters: mode diameter, geometric standard deviation and concentration (area under the curve). The size distribution reconstructed from the fitted lognormals is shown in Figure 3c.

We have made a comparison to another new inversion program by Dzubay and Hasan (1989). Their procedure assumes a priori that the size distribution consists of lognormal modes. The data are inverted and fitted in one step. We have used their program to analyze all of our nitrate data taken at Claremont during the summer period, a total of 44 size distributions. In their program, it is

necessary to restrict the number of free parameters. In the case of a trimodal fit, we specified the geometric standard deviation of the smallest mode.

The results for the lognormal parameters are compared to those obtained from our inversion and fitting program in Table 1. The agreement is excellent for all of the parameters, the differences being well within the uncertainties. It should be noted that the standard deviation listed with each quantity in Table 1 is a measure of the spread of the data and not the error. When a bimodal fit was specified, unrealistically large geometric standard deviations were obtained from the Dzubay and Hasan program and the goodness of fit evaluated from Chi square was poor, whereas it was excellent for the trimodal fit. This reinforces the finding by our inversion procedure that the distributions are trimodal. It is also significant that the geometric standard deviations produced by the two programs are in good agreement. Neither program involves any smoothing. In routines which use smoothing, the degree of smoothing affects the sharpness of the peaks in the distribution. It is worth noting that the above comparisons were made with common inputs for the impactor efficiency functions and the estimated stage mass errors, to which both inversion programs are sensitive.

RESULTS

Particle Size Distributions

A total of 900 particle size distributions for sulfate, nitrate, ammonium, sodium and chloride ions were obtained. As examples, some nitrate distributions from Claremont during summer SCAQS are shown in Figure 4. The distribution for the morning period beginning at 0600 on July 13, 1987, is the same as that in Figure 3. It can be seen that the two submicron modes decay during the day and the coarse mode dominates the last two periods. Also, the inversion detects the smaller of the two submicron modes even at low concentration. Other examples, in Figure 5, are sulfate distributions from Long Beach during summer SCAQS. The typical sulfate distribution during SCAQS is dominated by a $0.7 \mu\text{m}$ mode and has lesser amounts in a mode at $0.2 \mu\text{m}$ and in a coarse mode. An atypical example of a sulfate distribution is shown among the distributions in Figure 6. On September 2 at Rubidoux, the $0.2 \mu\text{m}$ mode dominates the first two periods, but during the last two periods the bulk of the concentration shifts into the larger of the two submicron modes.

Figure 7 displays examples of ammonium size distributions from Claremont during summer SCAQS. Since ammonium is associated with both sulfate and nitrate, the ammonium size distributions are composites of those of sulfate and nitrate. The distributions on June 19 have considerable concentrations in the coarse mode.

The parameters of the fitted lognormals contain essentially all of the information in the size distributions. Therefore, plots of the mode parameters can display the systematic characteristics of the size distributions. In Figure 8,

mode concentrations are plotted vs. mode diameters for all stations and all sampling periods during summer SCAQS. In the left column, absolute mode concentrations are plotted, while in the right column, relative mode concentrations are plotted. Relative mode concentrations are the fraction of the total concentration in the mode. It is evident that the size distributions for sulfate, ammonium and nitrate consist of three modes, two submicron and one supermicron.

The relative mode concentration plot for sulfate (Figure 8d) is especially striking. The points cluster into the three modes, showing little difference with sampling period or sampling site. The plot for ammonium (Figure 8e) is similar. For nitrate (Figure 8f), however, the concentrations of the two larger modes are spread out. In Figure 9, the summer data for nitrate are plotted separately for the three sites. Beginning with Long Beach (Figure 9a), most of the concentration is in the coarse mode, probably because the coastal location promotes the reaction of nitric acid with sea salt (Wall et al., 1988). In Figure 9b, the nitrate plot for Claremont, the percentage of the concentration in the coarse mode has decreased while the percentage in the larger of the two submicron modes has increased. This reflects the growth in concentration of the submicron mode by contributions from additional emission sources as the aerosol is transported inland and the accumulation of the product of photochemical reactions. The plot for Rubidoux (Figure 9c) shows a continuation of the same trend, with the submicron mode now dominant. Since there are major sources of ammonia between Claremont and Rubidoux, nitric acid will be converted to ammonium nitrate during transport between the two sites, further enhancing the fine nitrate at Rubidoux.

Mode data from fall SCAQS are plotted in Figure 10. The patterns are qualitatively similar to those of summer SCAQS data. While the points appear to have more scatter, for the most part they lie within the envelope of the points on the summer data plots. Part of the impression of more scatter is due to the lower density of points owing to the fewer sampling days during the fall.

To examine the particle diameters of the modes, it is useful to plot the frequency of occurrence of the modes vs. mode diameter, as in the left column of Figure 11. Again, three modes are seen in the plots for sulfate, nitrate and ammonium. The two submicron modes peak at approximately 0.2 and 0.7 μm . Another aspect of the data can be examined by plotting the average mode concentration vs. mode diameter. This is shown in the right column of Figure 11. For sulfate (Figure 11d), the average mode concentration rises with increasing mode diameter from 0.1 μm up to just above 1 μm . In the size range 0.3-0.4 μm , the gap between the two submicron modes is evident. Above 1 μm there is an abrupt fall in the mode concentration to nearly zero. The mode diameter where this upper edge of the sulfate distribution occurs varies systematically from approximately 0.8 μm at Long Beach to 1.0 μm at Claremont and to 1.2 μm at Rubidoux. This implies continued growth of the sulfate-containing particles during transport across the Los Angeles basin from the coast. The mode concentration plot for nitrate (Figure 11f) has a much different appearance from that for sulfate. The submicron nitrate concentration peaks at about 0.5 μm . This point will be discussed below.

Figure 12 is similar to Figure 11, but for sodium, chloride and total ionic mass. Sodium (Figure 11a,d) is seen to be almost entirely in the coarse mode as expected from its sources, sea salt and wind-blown dust. Chloride (Figure 12 b,e) also has a strong coarse mode as expected from sea salt, but there is

a significant amount in the larger of the two submicron modes from an unknown source. The small amount in the smaller of the two submicron modes should be regarded with reservations because of analytical difficulties, discussed below.

In order to derive mass-weighted averages for the mode parameters, the mass size distributions for nitrate, sulfate, ammonium and sodium were summed and the resulting total distributions were fitted with lognormal functions. The frequency of the modes is plotted vs. mode diameter in Figure 12c. The averages of the mode parameters of the mass distributions are listed in Table 2. The submicron mode with mean aerodynamic diameter of $0.2 \mu\text{m}$ has been labelled "condensation" mode and the $0.7 \mu\text{m}$ mode has been labelled "droplet" mode. This terminology anticipates our interpretation of the data which will be presented below. The terminology is convenient since 0.2 and $0.7 \mu\text{m}$ are only the most probable diameters of the two submicron modes. In Table 2, the considerable standard deviations of the diameters reflect the dispersion of the data and not the uncertainties, which were smaller. We note that the mean diameters of the two submicron modes were the same during the summer and fall SCAQS periods. Also, the mode geometric standard deviations were nearly identical for the summer and fall periods. The present mass distributions do not include the organics and the trace metals; however, the inorganic ions account for a large fraction of the fine particle mass as verified by a very limited examination of preliminary SCAQS data from several groups.

Mode frequencies and average mode concentrations are plotted vs. mode diameter in Figure 13 for fall SCAQS data. The plots are similar to their counterparts for summer SCAQS data, but there is considerable "noise" in the the frequency plots below one micron due to the low number of events.

Aerosol Composition and Concentration

Ion balances were examined by integrating the size distributions of the ion concentrations over appropriate particle size ranges. In Figure 14a, the ammonium concentration is plotted vs. the sum of nitrate and sulfate for the size range 0.05 - 0.4 μm , corresponding to the approximate size range of the condensation mode. The correlation is excellent and there is only a small (8%) excess of ammonium. The correlation is similar in the size range 0.4 - 2.0 μm (Figure 14b), corresponding to the droplet mode. Sodium and chlorine ions were not included in these plots because the sodium concentration (in equivalents/ m^3) is only 1% of the total submicron ion concentration and chloride is only 3.5%. Further, the chloride concentrations are less reliable than the others because of analytical difficulties. Polar organic compounds interfered with the ion chromatography for chloride. In approximately 40% of the samples, chloride determination was possible only after some of the organics had been removed by extraction with cyclohexane. This experience implies that there were high concentrations of organic acids in the aerosol during SCAQS.

The near-balance of ammonium with sulfate and nitrate implies that the submicron aerosol was almost neutral. Unfortunately, the pH measurements did not produce useful data because of the small sample obtained with four hour impactor sampling, low aerosol acidity and the relatively high blanks. In previous sampling for longer time periods we have found low strong acidity in this air basin (John et al., 1988).

The impactor substrates were visually inspected when they were removed from the impactor. During summer SCAQS, 31% of the samples from stage 3 (geometric

mean particle diameter $0.37 \mu\text{m}$) and 32% of the samples from stage 4 ($0.74 \mu\text{m}$) showed evidence that the particle deposit had been wet. During the fall, the corresponding percentages were 25% and 21%. Only a few cases were noted on stages 2 ($0.19 \mu\text{m}$) and 5 ($1.5 \mu\text{m}$). This is direct evidence that droplets were being sampled in the size range of the $0.7 \mu\text{m}$ mode.

In Figure 14c, cation vs. anion concentrations are plotted for the size range $2.0 - 15 \mu\text{m}$, corresponding to coarse mode particles. While the correlation is good, there is a 17% deficiency in cations. Using our partial data set for Mg^{++} and Ca^{++} ions on stages 6 and 7, we can examine the ion balance for the approximate size range $2.2 - 8.2 \mu\text{m}$. With the addition of Mg ions, there remains a deficiency of cations. Adding both Mg^{++} and Ca^{++} ions brings the cations and anions nearly into balance at Long Beach during the summer. For Claremont and Rubidoux during the summer, and for Long Beach and Los Angeles during the fall, adding both Mg and Ca ions results in a cation/anion ratio of approximately 1.3, with a large variation from period to period. Evidently there are significant missing ions in the coarse fraction. The nearly exact ion balance over the entire particle size range (Figure 14d) is due to the fortuitous cancellation of the ion imbalances in the fine and coarse particle ranges.

It has already been mentioned that coarse nitrate is probably produced by the reaction of nitric acid on coarse sea salt particles, producing sodium nitrate. However, the amount of coarse ammonium is greater than the amount of sulfate (in equivalents) at Claremont and Rubidoux. The excess ammonium is probably associated with some of the nitrate. Wall, et al.(1988) discussed the possibility that ammonia could react with nitric acid on the surface of wet

marine aerosol. Alternatively, ammonium nitrate might be a component of wind-blown soil. Coarse sulfate from natural sources, whether sea salt or soil, will be correlated with coarse sodium. For a sea salt source, the slope of the regression line would be 0.12 and for soil the slope would be larger. On this basis the proportion of sea salt was highest at Long Beach and that of soil was highest at Rubidoux.

In Figure 15, nitrate concentrations integrated over the particle size ranges corresponding to the three modes are plotted vs. sampling periods during summer SCAQS. The two fine particle mode concentrations show regular diurnal variations with midday peaks. Both the peak heights and the peak times increase systematically in going eastward from Long Beach to Claremont and then to Rubidoux. While the condensation mode and the droplet mode plots are similar, there are some differences in detail. On the other hand, the coarse mode concentration shows different dependences on location and time from those of the fine particle modes, implying that the coarse mode is formed by different processes than the fine modes. The coarse mode data for all three stations show similar time dependence, with nearly the same concentrations at Claremont and Rubidoux, and lower concentrations at Long Beach.

The time series for sulfate mode concentrations, plotted in Figure 16, do not show the regularity exhibited by the nitrate concentrations. For the condensation mode, the timing of peak concentrations varies, with some tendency to occur in midday or the afternoon, and to occur earlier at Long Beach than at the inland stations. The pattern for the droplet mode is different from that of the condensation mode. The Claremont and Rubidoux data track each other, but the Long Beach data differ substantially, perhaps because of the stationary sources of sulfur dioxide in the Long Beach area and possibly because of

the influence of relative humidity on the formation of the droplet mode, discussed in detail below. Coarse mode concentrations are similar at the three stations; Rubidoux is occasionally higher.

In Figure 17, the time series for nitrate concentrations during fall SCAQS are plotted for the particle size ranges of the three modes. In all three size ranges the data from the Los Angeles and Long Beach stations track each other fairly well, with no major difference in concentrations. There is a diurnal variation, with some tendency for the peaks at Los Angeles to lag those at Long Beach.

The sulfate time series for fall SCAQS are shown in Figure 18. In the condensation mode size range, the sulfate concentration tends to be maximum at midday at both stations. The droplet mode pattern is less regular. The coarse mode concentrations are low except for the peak on November 12.

It has been possible to present here only a small portion of our data. A complete data set as well as hard copy of tables and plots is in the SCAQS data bank maintained by the Research Division of the California Air Resources Board, P. O. Box 2815, Sacramento, CA 95812.

DISCUSSION OF THE FINE PARTICLE MODES

The data presented above show that the fine particle sulfate, nitrate and ammonium occur in two lognormal modes, one with a most probable aerodynamic diameter of $0.2 \mu\text{m}$ and the other with a diameter of $0.7 \mu\text{m}$. Hering and Friedlander (1982) reported sulfur modes with mass median aerodynamic

diameters 0.20 and 0.54 μm . Their Figure 4, in which the impactor stage masses are plotted vs. diameter, shows that the composite size distribution for the larger of the two modes includes a substantial amount of the smaller mode. Inclusion of the small diameter tail of the distribution undoubtedly biased the mass median diameter to smaller size. The geometric mean diameters of particles on the two peak stages are 0.18 and 0.71, based on the cutpoints listed by Hering and Friedlander (1982), and are in excellent agreement with our mode diameters. We conclude that we have seen the same mode structure in the aerosol as did Hering and Friedlander. They concluded, on the basis of aerosol growth dynamics, that the 0.2 μm mode was formed by gas phase oxidation of sulfur dioxide and the 0.7 μm mode by droplet phase reactions. The droplet phase reactions were assumed to occur in preexisting liquid aerosol particles in an urban accumulation mode with a geometric volume mean diameter of 0.32 μm , as given by Whitby and Sverdrup (1980). Assuming a density of 1.5, 0.32 μm geometric diameter corresponds to 0.39 μm aerodynamic diameter. However, we have found essentially all of the fine inorganic particle mass in the 0.2 and 0.7 μm modes, i.e., there is no accumulation mode at the typical Whitby particle diameter.

Figure 11d suggests that the larger of the two fine particle modes might grow out of the smaller one. To examine this possibility, mode concentration is plotted vs. mode diameter for sulfate sampled at Claremont during summer SCAQS in Figure 19. The data points cluster into the two submicron modes, each with a trend of increasing concentration with increasing diameter. The lines are drawn through the clusters with a slope corresponding to a diameter cubed law, i.e., volume growth at constant particle number. The relative constancy (on a log-log scale) of particle number could have resulted from the selection of

SCAQS intensive study days according to uniform criteria and the relative constancy of source emissions. The data points are an ensemble of measurements made during various sampling periods and therefore represent the modes in various stages of growth. The concentration of the smaller mode increases to a maximum of about 50 neq/m^3 (indicated by the horizontal dashed line) and the concentration of the larger mode starts at about this concentration. This strongly suggests that the growth of the larger mode is a continuation of growth in the smaller mode. There is apparently a transition in the vicinity of the dashed line where a large growth in diameter occurs with relatively small growth in sulfate concentration. This could be explained by assuming that the particles in the smaller mode are dry and that some of them are nucleated and then make the transition to the larger mode mainly by water condensation. The transition takes place from the large particle end of the smaller mode; this is consistent with the smaller critical supersaturation associated with larger particle size due to the Kelvin effect.

There are only a few data points in the gap between the modes. This indicates that the transition occurs rapidly compared to our 3.5 hr. sampling period. There is a remarkable set of data points spanning the transition which have been replotted in Figure 20 for clarity. From left to right, these data were taken successively during the four sampling periods on September 2 and the first three sampling periods of September 3. During this sequence, the mode diameter increased monotonically. The sequence began on September 2, by far the driest day during the SCAQS study, with a relative humidity (RH) which dropped almost to 20%. Evidently the low RH slowed the droplet growth so that points during the transition could be sampled. While the transition was made at relatively constant sulfate concentration on the log-log plot of Figure 14, the sulfate concentration actually increased by a factor of about 2.5. When

the sulfate data for Long Beach and Rudidoux were plotted, the results were similar to Figure 19 for Claremont, with the two modes showing approximately cube law growth, but there were almost no data points in the transition region, even on September 2. The unique transition events at Claremont were evidently produced by atmospheric conditions which differed slightly from those at the other stations.

During the transition episode at Claremont, September 2-3 (Figure 20), the nitrate droplet mode diameter was the same, within experimental error, as the sulfate mode diameter for each sampling period, the average difference being only $0.06 \mu\text{m}$. Therefore, the nitrate was in the same particles as the sulfate. However, the nitrate mode concentration varied over a wide range essentially independent of the sulfate mode concentration. This shows that droplet growth was determined by the accrual of sulfate and water. We have noted (Figure 11f) that the nitrate mode concentration for all the summer data peaked near $0.5 \mu\text{m}$. In fact, for a droplet mode diameter of $0.70 \mu\text{m}$ and a geometric standard deviation of 1.7, the surface mode diameter is $0.53 \mu\text{m}$. The nitrate-forming reaction apparently depends on the droplet surface. The acidification of the droplets by reaction with gaseous nitrogen or sulfur species is followed by reaction with ammonia gas since the ion concentrations are nearly balanced (Figure 14).

Because the RH during the morning and night periods averaged 20-25% higher than the two daytime periods, the data were examined for any effect on the droplet mode diameter. At Long Beach, the sulfate droplet mode diameter averaged $0.1 \mu\text{m}$ larger during the morning and night periods than during the daytime periods, both in the summer and in the fall. No such difference was

found at Claremont or Rubidoux. The ability to detect an effect of RH was probably limited by the long sampling times, especially the overnight period.

McMurry and Wilson (1983) observed particle growth rates downwind of Columbus, Ohio using an electrical mobility analyzer and an optical counter. The data were accounted for by growth law theory which gives particle diameter growth rates by condensation (due to gas phase reactions) dominating at small diameters but decreasing with particle size. Droplet phase reactions have growth rates which increase rapidly with particle size, eventually dominating over gas phase reaction rates. Our finding that the sulfate concentration is highest in the droplet mode is consistent with the growth law theory. It is also significant that aerosol sulfur size distributions measured by McMurry and Wilson in Ohio were very similar to those of Hering and Friedlander for the Los Angeles basin.

The above discussion leads to the identification of the 0.2 μm mode as a condensation mode containing gas phase reaction products. Some of the particles in this mode apparently nucleate and grow into the 0.7 μm mode, for which the name "droplet mode" is proposed. The proportion of mass in the two modes depends on atmospheric conditions. These two fine particle modes are believed to be general features of the atmospheric aerosol, not just in Los Angeles. This constitutes a revision of the Whitby model, which was based on transformed number distributions. Additional uncertainty was introduced by the data from measurements with an Electrical Aerosol Analyzer and an optical particle counter, with a division of the particle size range at approximately 0.5 μm , aerodynamic diameter, between the two instruments. There was also possible evaporation of water from the particles in the sampling line (Sverdrup and Whitby, 1980). Thus the experimental method was probably not capable of

resolving the two modes detected in the present work with a single instrument measuring chemical mass.

The new model of the structure of the atmospheric fine particles, with a condensation mode and a droplet mode, can be expected to lead to new interpretations of the effects of the aerosol. For example, since the droplet mode has a most probable aerodynamic diameter of $0.7 \mu\text{m}$, near the peak diameter of the light scattering curve, visibility reduction will be highly dependent on the mass in this mode.

CONCLUSIONS

The particle size distributions of the inorganic ions were measured over the size range from $0.075 - 16 \mu\text{m}$ during SCAQS. The distributions can be completely characterized by three lognormal modes, one at $0.2 \pm 0.1 \mu\text{m}$ which is probably a condensation mode containing gas phase reaction products, one at $0.7 \pm 0.2 \mu\text{m}$ identified as a droplet mode, and a coarse mode. Evidence was obtained that the droplet mode grows out of the condensation mode by the addition of water and sulfate. Nitrate was internally mixed with sulfate in the droplet mode. In both the condensation and droplet modes, the sulfate and nitrate ion equivalents were nearly balanced by ammonium ions. Most of the inorganic ion mass was in the droplet mode during SCAQS except during a period of exceptionally low humidity. Since most of the fine particle mass is included in the ions analyzed, the observed condensation and droplet modes characterize the overall size distribution in the $0.1 - 1 \mu\text{m}$ range, previously described by Whitby as a single accumulation mode.

RECOMMENDATIONS

At the time this report was written, only a very limited amount of information from the other SCAQS participants was available to the authors. When the other experimental groups have reported their results, there will be an obvious need to develop an integrated data interpretation. At the first level, impactor data on organics and on elements can be combined with the present data on inorganic ions. For example, it is possible that some of the droplet mode particles result from the nucleation of elemental carbon particles in the condensation mode. The growth of these particles by the addition of sulfate and water would carry the carbon "seed" particles up into the droplet mode. This concept can be tested with the data. At the next level, there are other data on particles taken with filter samplers, etc. Finally, there is a very large amount of data on other pollutants and on meteorology which can be used in interpreting the data.

It should be emphasized that the interpretation of all the SCAQS aerosol data needs to be made within the framework of the present new model of the particle size modes. For example, visibility reduction will be almost entirely determined by light scattered by droplet mode particles. The most probable size of the droplet mode is $0.7 \mu\text{m}$, aerodynamic diameter, which is near the peak of the light scattering curve. However, the droplet mode extends from about $0.4 \mu\text{m}$ to above $1 \mu\text{m}$. The growth of the mode depends on atmospheric conditions. The effect on visibility will also vary accordingly.

The present findings open many important new questions for research. For example, how does the droplet mode grow out of the condensation mode? Which particles get nucleated? When are they nucleated during the day and how are

they nucleated? What is the mechanism for nitrate formation in the droplet mode? Answers to these questions are needed for an understanding of how the atmospheric aerosol is formed. In turn, the knowledge can be used as the basis for more effective control strategies.

ACKNOWLEDGEMENTS

We thank Dr. Hwa-Chi Wang for his assistance in operating the impactors. We also thank Dr. Thomas Dzubay for making his data inversion program available to us. Helpful discussions were held with Dr. Peter McMurry and Dr. Susanne Hering.

This report was submitted in fulfillment of ARB Contract Number A6-112-32, "Acidic Aerosol Size Distributions During SCAQS" by the California Public Health Foundation under the sponsorship of the California Air Resources Board. Work was completed as of August, 1989.

REFERENCES

Appel, B.R., Kothny, E.L., Hoffer, E.M. and Wesolowski, J.J. (1980) Sulfate and Nitrate Data from the California Aerosol Characterization Experiment (ACHEX). In The Character and Origins of Smog Aerosols, G. M. Hidy, et al. ed., pp. 315-335, John Wiley and Sons, N.Y.

Durham, J.L. and Stockburger, L. (1986) Nitric Acid-Air Diffusion Coefficient: Experimental Determination". Atmos. Environ. 20, 559-563.

Dzubay, T.G. and Hasan, H. (1989) Deducing Aerosol Size Distribution Parameters from Cascade Impactor Data. Submitted to Aerosol Sci. Technol.

Hering, S. V. and Friedlander, S. K. (1982) Origins of Aerosol Sulfur Size Distributions in the Los Angeles Basin. Atmos. Environ. 16, 2647-2656.

John, W., Wall, S.M. and Ondo, J.L. (1988) A New Method for Nitric Acid and Nitrate Aerosol Measurement Using the Dichotomous Sampler. Atmos. Environ. 22, 1627-1635.

McMurry, P.H. and Wilson, J.C. (1983) Droplet Phase (Heterogeneous) and Gas Phase (Homogeneous) Contributions to Secondary Ambient Aerosol Formation as Functions of Relative Humidity. J. Geophys. Res. 88, 5101 - 5108.

Possanzini, M., Febo, A. and Liberti, A. (1983) New Design of a High-Performance Denuder for the Sampling of Atmospheric Pollutants. Atmos. Environ. 17, 2605-2610.

Sverdrup, G.M. and Whitby, K.T. (1980) The Effect of Changing Relative Humidity on Aerosol Size Distribution Measurements. In The Character and Origins of Smog Aerosols, G. M. Hidy, et al. ed., pp. 527-538, John Wiley and Sons, N.Y.

Wall, S.M., John, W. and Ondo, J.L. (1988) Measurement of Aerosol Size Distributions for Nitrate and Major Ionic Species. Atmos. Environ. 22, 1649-1656.

Wang, H.C. and John, W. (1988) Characteristics of the Berner Impactor for Sampling Inorganic Ions. Aerosol Sci. Technol. 8, 157-172.

Whitby, K.T. (1978) The Physical Characteristics of Sulfur Aerosols. Atmos. Environ. 12, 135-159.

Whitby, K.T. and Sverdrup, G.M. (1980) California Aerosols: Their Physical and Chemical Characteristics. In The Character and Origins of Smog Aerosols, G. M. Hidy, et al. ed., pp. 477-517, John Wiley and Sons, N.Y.

Winklmayr, W., Wang, H.C. and John, W. (1988) Adaption of the Twomey Algorithm to the Inversion of Cascade Impactor Data. Submitted to Aerosol Sci. Technol.

Table 1. Comparison of average mode parameters for nitrate size distributions, Claremont, summer SCAQS, obtained by the data inversion programs of Winklmayer et al. (1988) and Dzubay and Hasan (1989).

Parameter		Submicron 1 n = 28	MODE		Supermicron n = 40
			Submicron 2 n = 35		
Mode Diameter, Aerodynamic, μm	W. et al.	0.196 ± 0.037	0.73 ± 0.13		4.40 ± 0.64
	D. & H.	0.199 ± 0.034	0.74 ± 0.13		4.35 ± 0.71
Mode Geometric Standard Deviation	W. et al.	1.44 ± 0.11	1.68 ± 0.20		1.82 ± 0.12
	D & H	1.40*	1.59 ± 0.19		1.79 ± 0.15
Relative Mode Concentration	W. et al.	0.09 ± 0.04	0.43 ± 0.16		0.52 ± 0.16
	D. & H.	0.10 ± 0.04	0.40 ± 0.17		0.53 ± 0.17

*Fixed Constant (See Text)

Table 2. Average mode parameters for the summer and fall SCAQS periods obtained by fitting the summed mass distributions of the ionic species. Means and standard deviations are listed.

	Condensation	MODE Droplet	Coarse
Aerodynamic Diameter, μm	0.2 ± 0.1	0.7 ± 0.2	4.4 ± 1.2
σ_g	1.5 ± 0.2	1.7 ± 0.2	1.9 ± 0.3
Av. Concentration, $\mu\text{g}/\text{m}^3$	4 ± 5	26 ± 21	13 ± 7
.....			
	Summer		
	Fall		
Aerodynamic Diameter, μm	0.2 ± 0.1	0.7 ± 0.3	5.5 ± 0.7
σ_g	1.5 ± 0.2	1.9 ± 0.5	1.8 ± 0.4
Av. Concentration, $\mu\text{g}/\text{m}^3$	9 ± 8	40 ± 29	5 ± 4

Table 3. Mean concentrations by mode in $\text{neq. m}^{-3} \pm \text{std. dev.}$

Mode *	NH_4	NO_3	SO_4	Na	CL
Summer SCAQS - Long Beach, Claremont, Rubidoux					
Condensation	75 ± 84	50 ± 90	24 ± 18	10 ± 0	10 ± 14
Droplet	352 ± 283	219 ± 238	129 ± 66	--	21 ± 12
Coarse	64 ± 50	128 ± 75	29 ± 14	72 ± 42	29 ± 23
Fall SCAQS - Long Beach, Los Angeles					
Condensation	140 ± 114	77 ± 76	26 ± 23	--	13 ± 11
Droplet	569 ± 404	425 ± 344	101 ± 58	--	33 ± 32
Coarse	42 ± 32	62 ± 45	12 ± 5	34 ± 21	16 ± 10

*For mode diameters see Table 2.

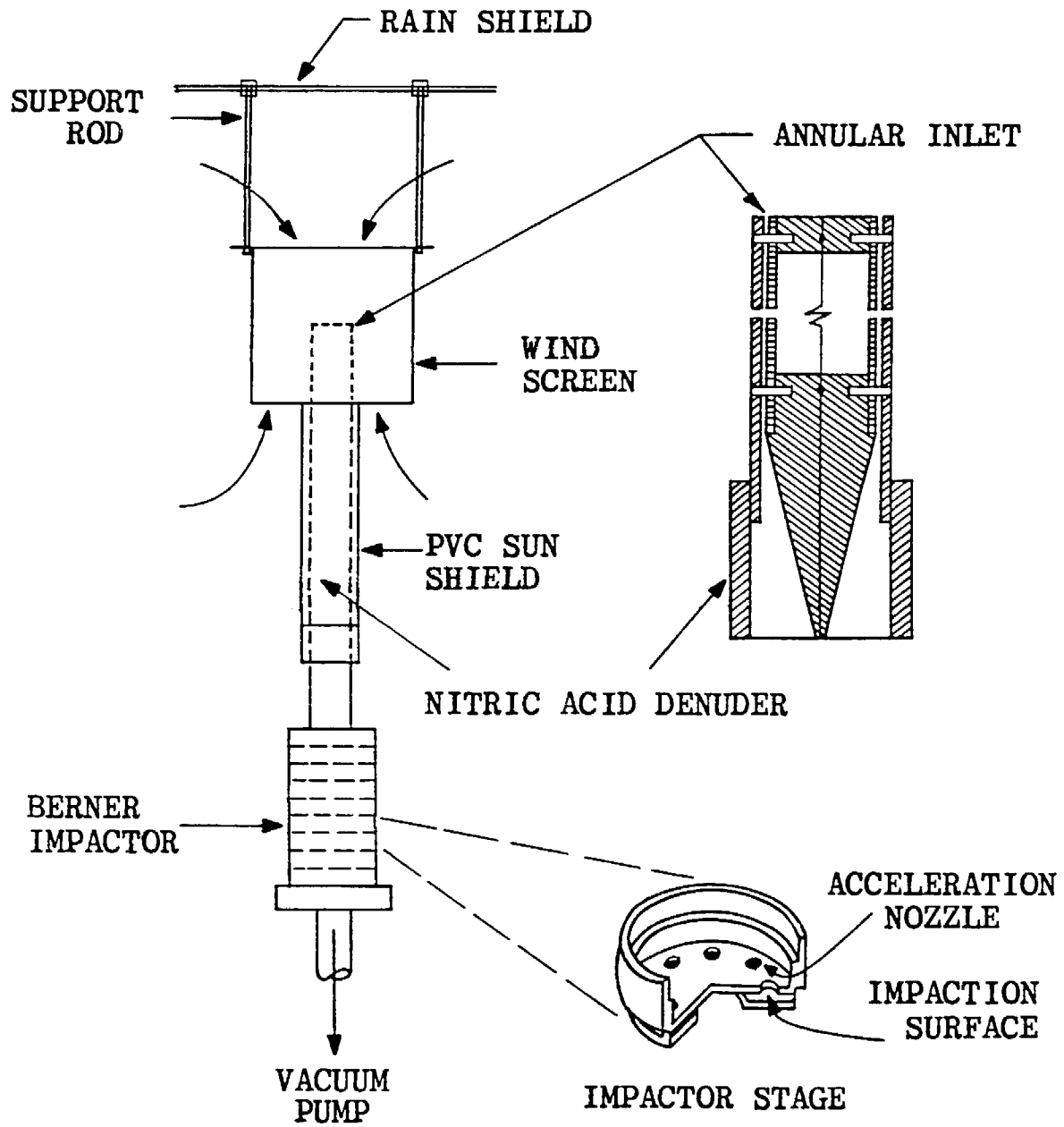


Figure 2. Diagram of sampling assembly.

Claremont N03 13-JUL-87 0600 - 0930

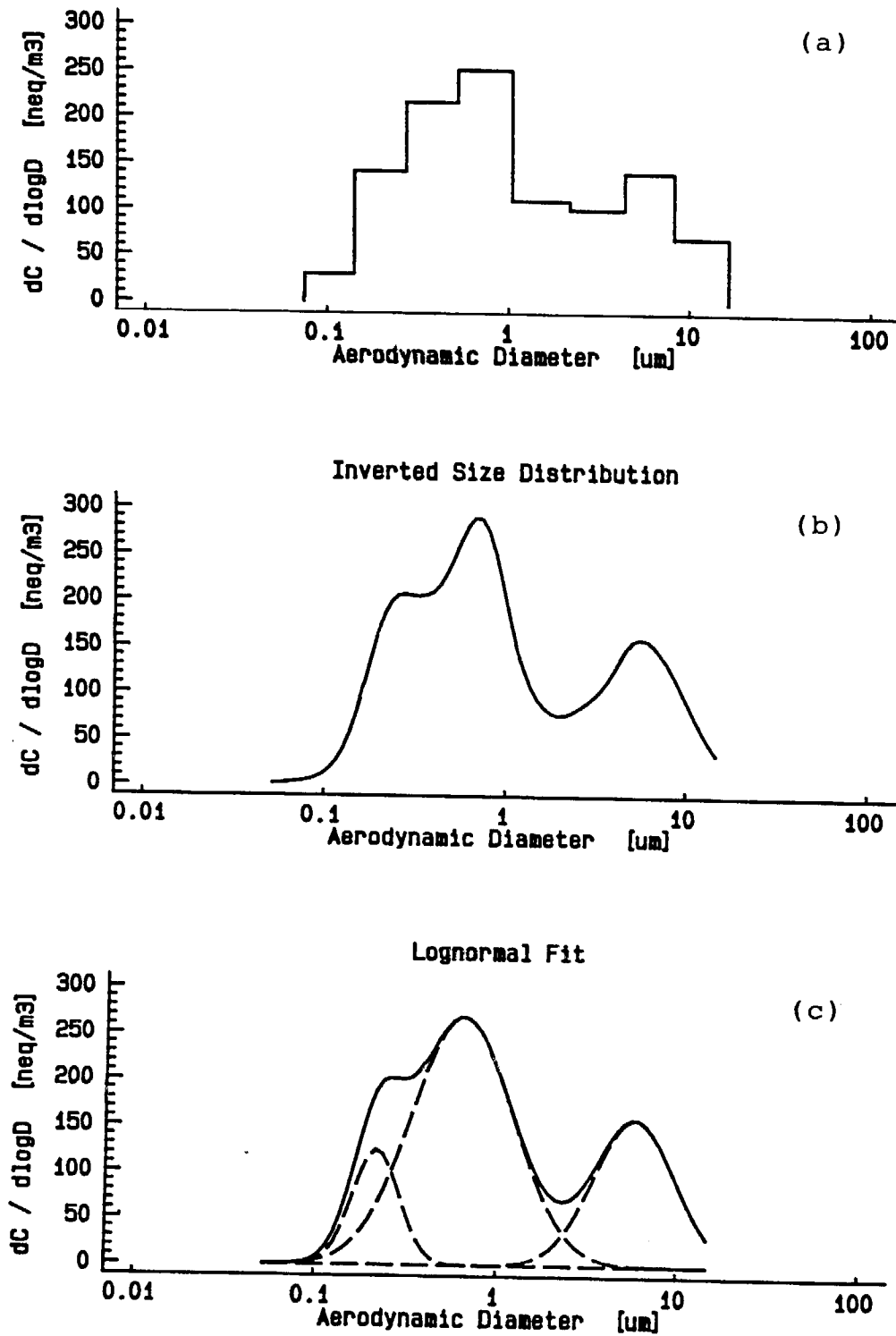


Figure 3. Example of impactor data analysis: (a) stage concentrations, (b) inverted size distribution, (c) solid line, distribution obtained by fitting a sum of lognormal functions to the inverted distribution; dashed lines, the lognormal functions.

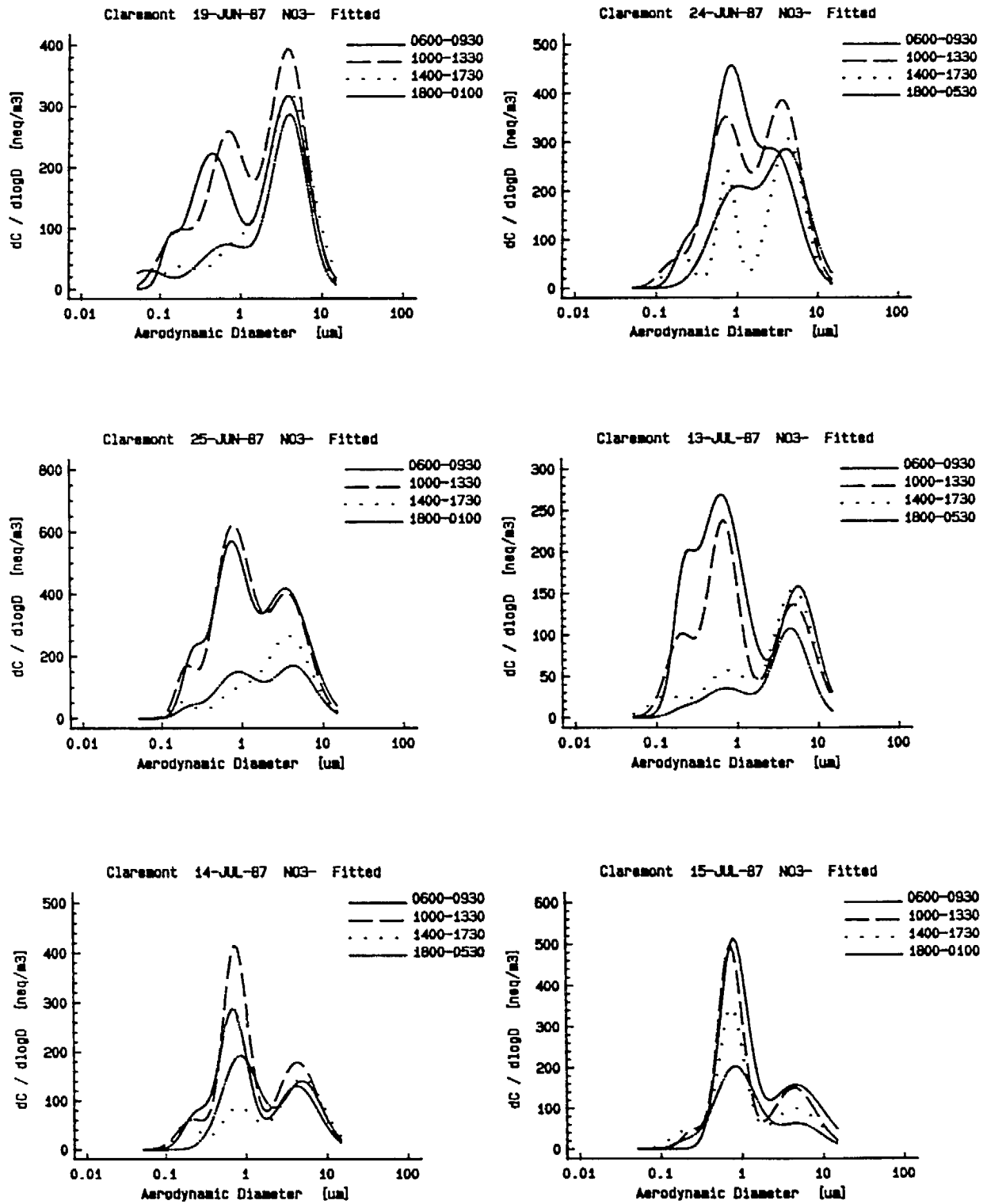


Figure 4. Examples of nitrate size distributions from Claremont during summer SCAQS. The data were processed as in Figure 3(c).

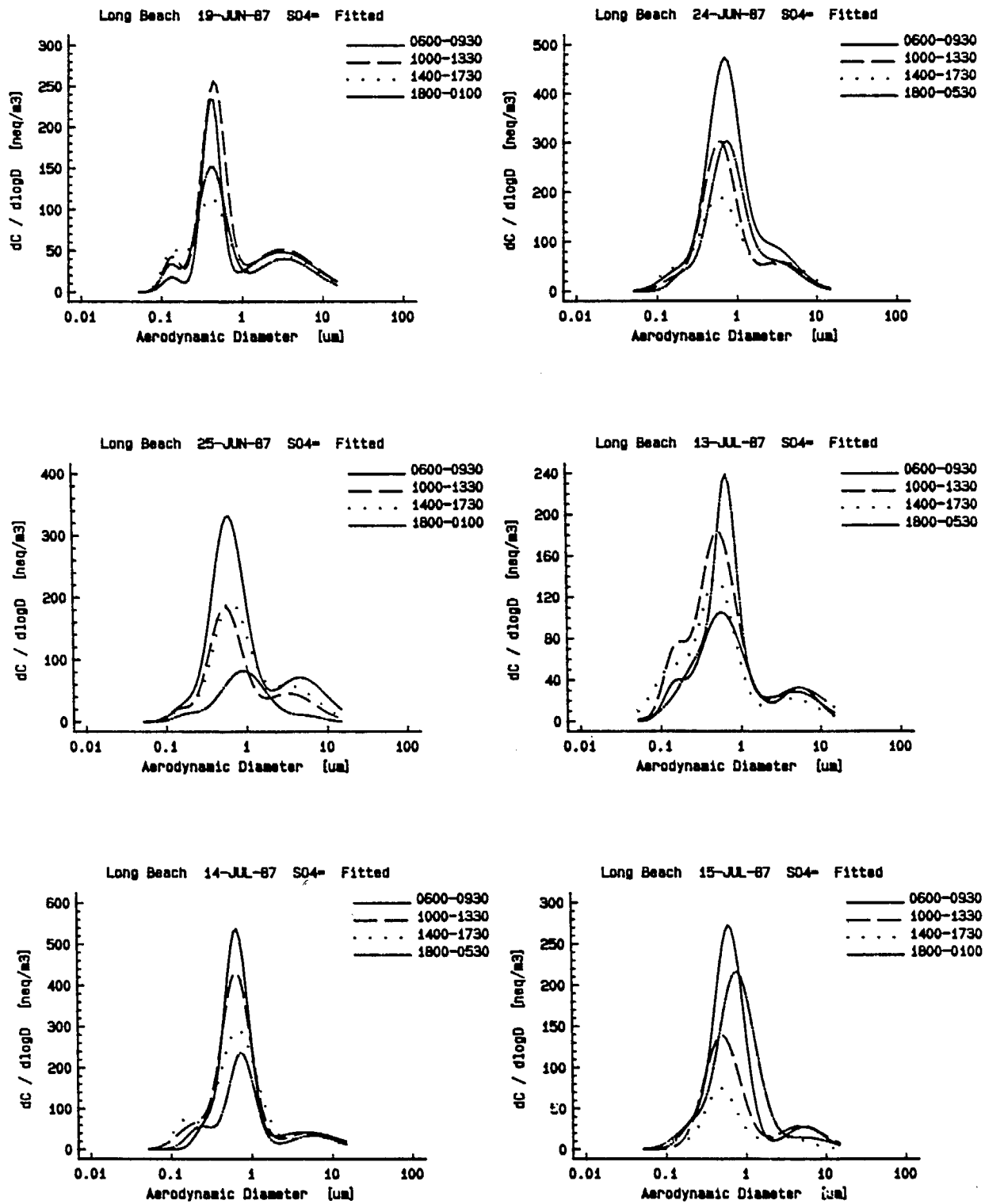


Figure 5. Sulfate size distributions from Long Beach during summer SCAQS.

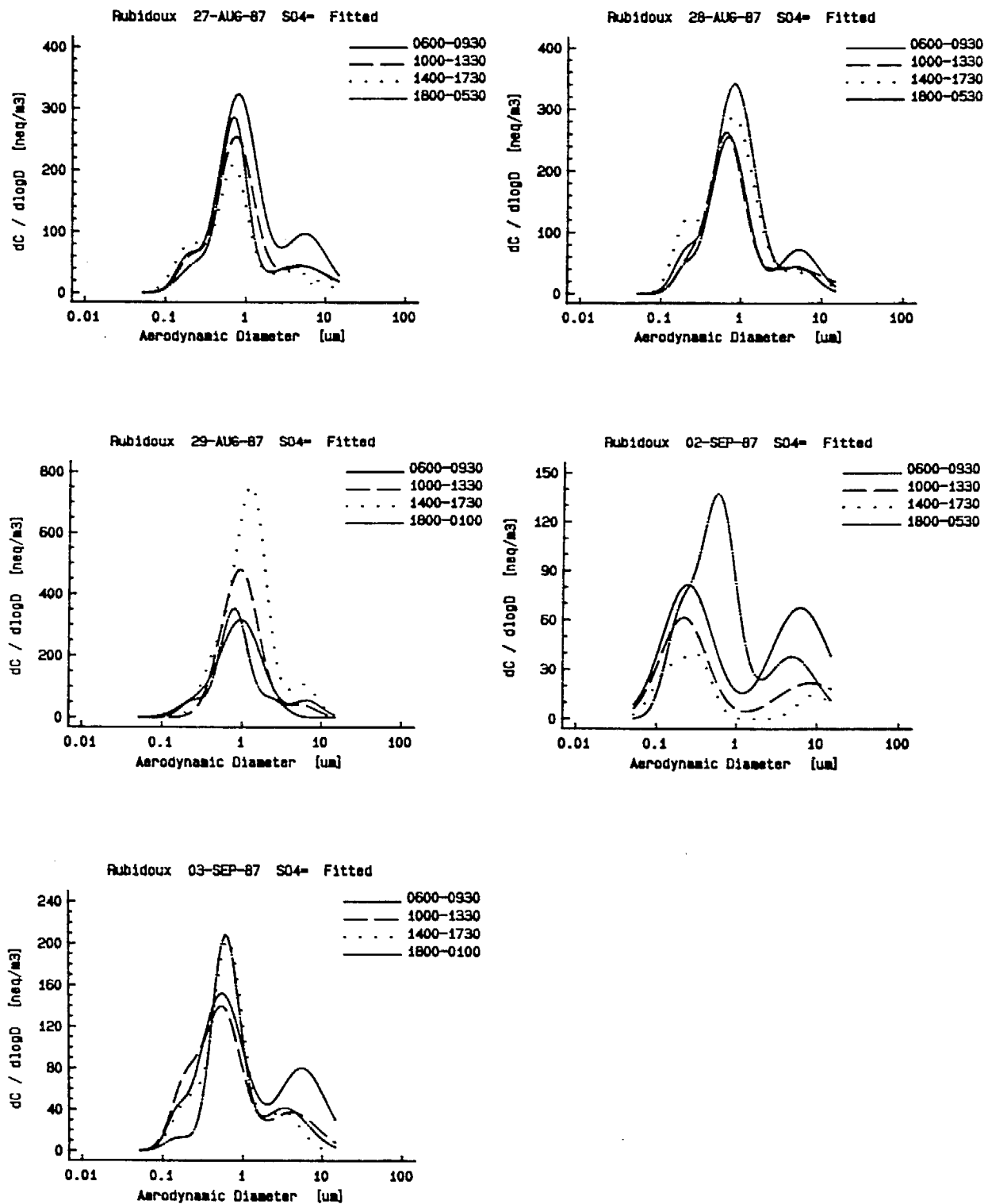


Figure 6. Sulfate size distributions from Rubidoux during summer SCAQS.

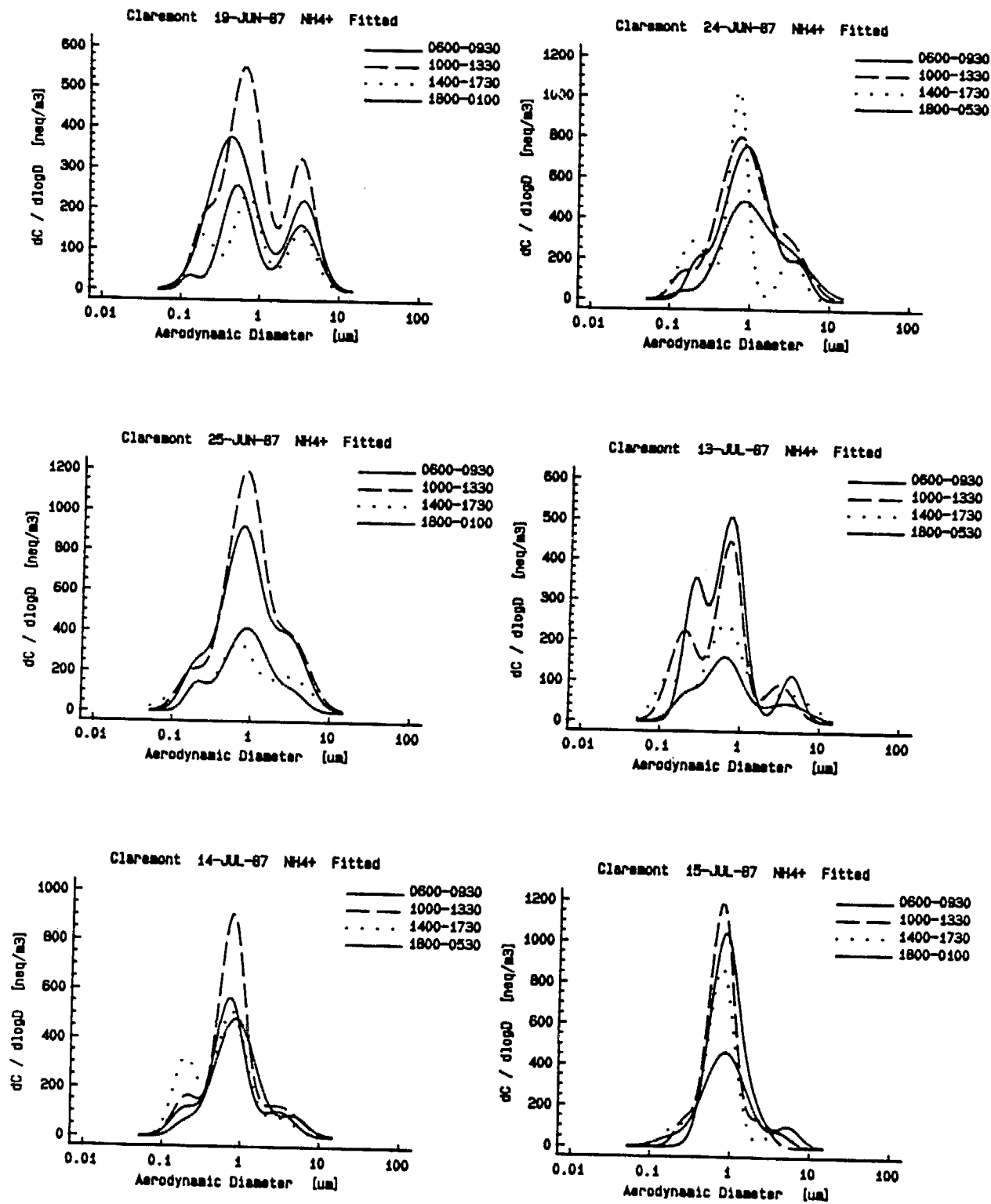


Figure 7. Ammonium size distributions from Claremont during summer SCAQS.

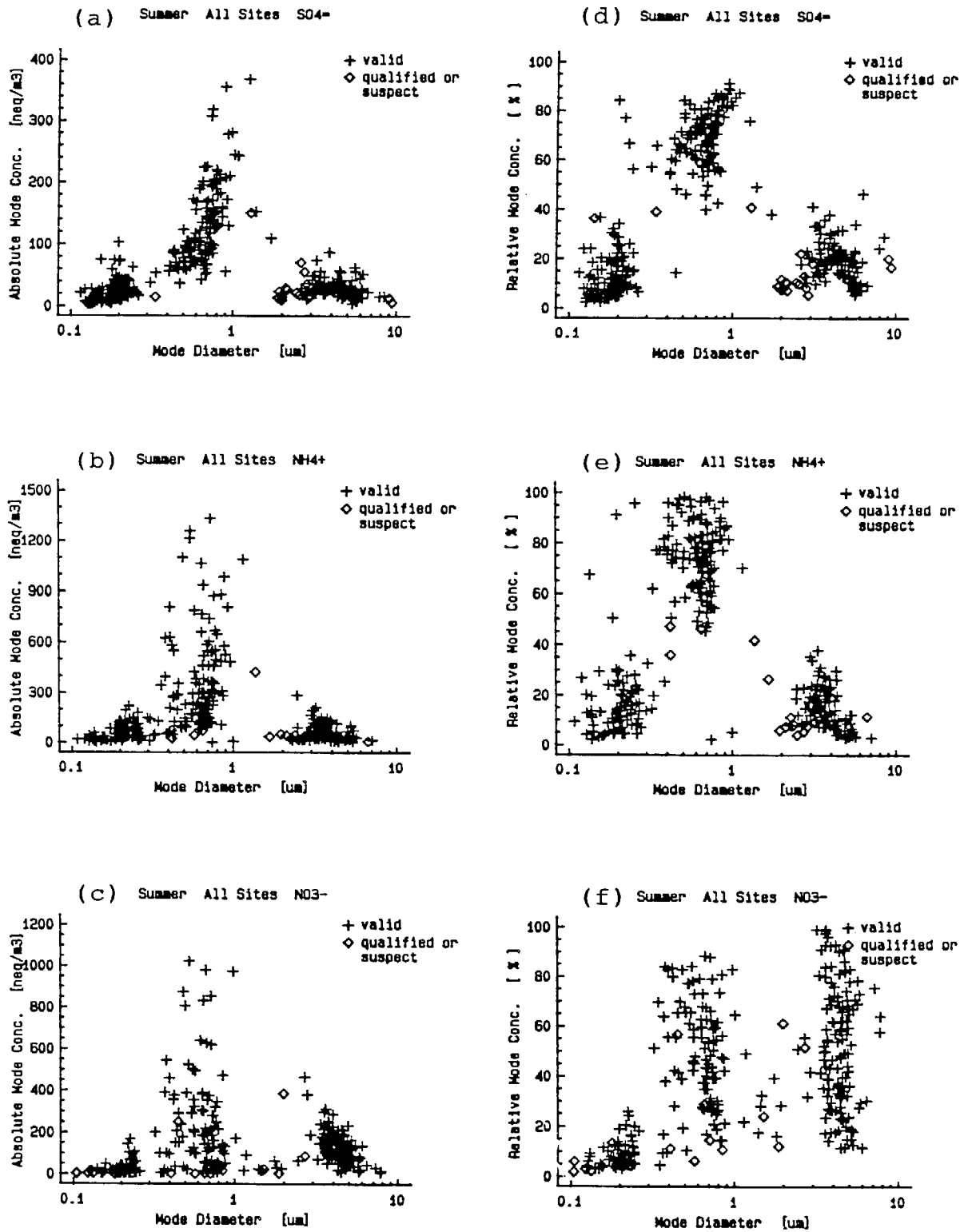


Figure 8. Mode concentrations vs. mode diameter for all sampling sites and all sampling periods during summer SCAQS: Left column, absolute mode concentrations; right column, relative mode concentrations.

SUMMER NO3-

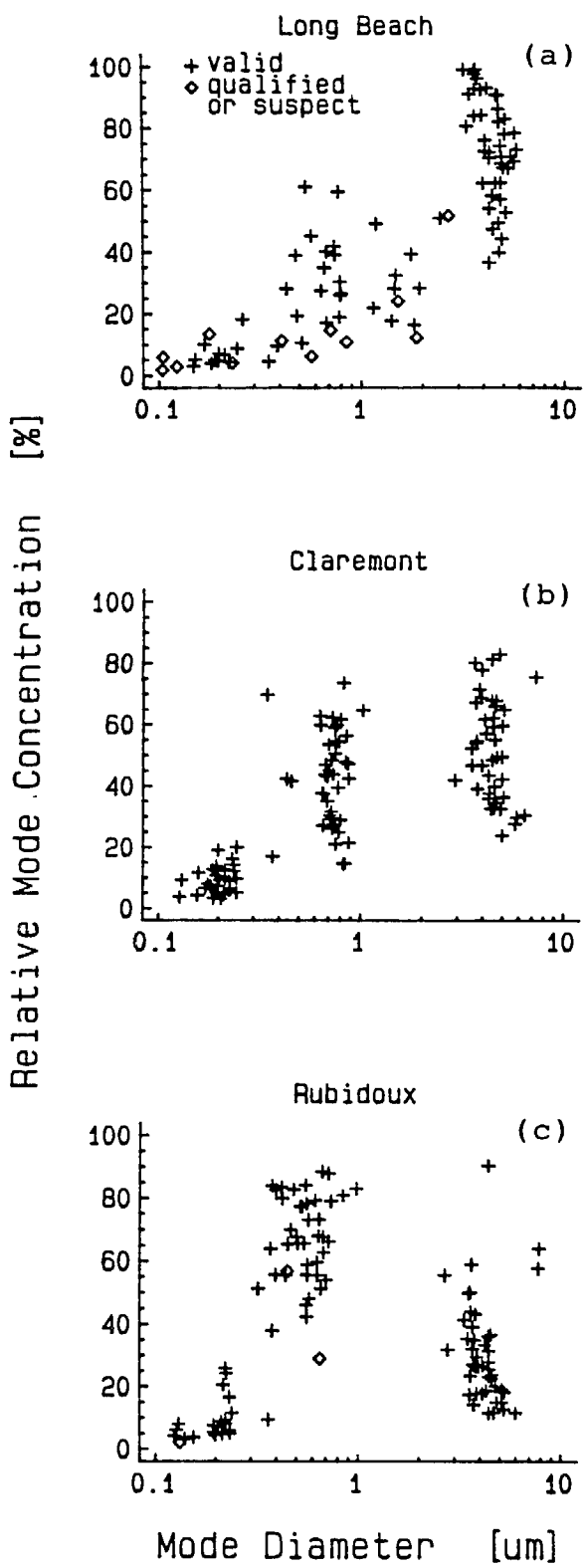


Figure 9. Relative mode concentration of nitrate vs. mode diameter for all sampling periods during summer SCAQS, from (a) Long Beach, (b) Claremont and (c) Rubidoux.

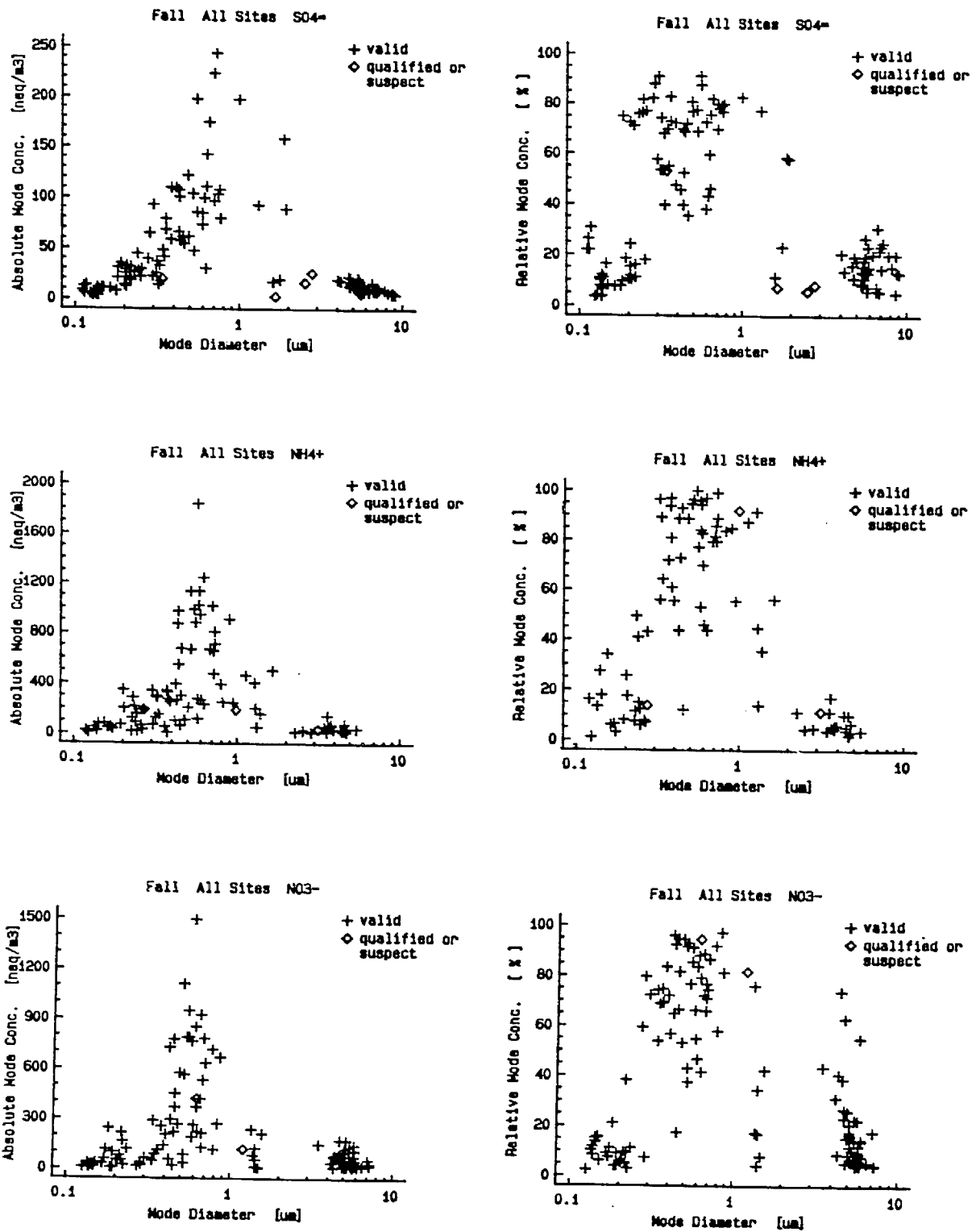


Figure 10. Mode concentrations vs. mode diameter for all sampling sites and all sampling periods during fall SCAQS: Left column, absolute mode concentrations; right column, relative mode concentrations.

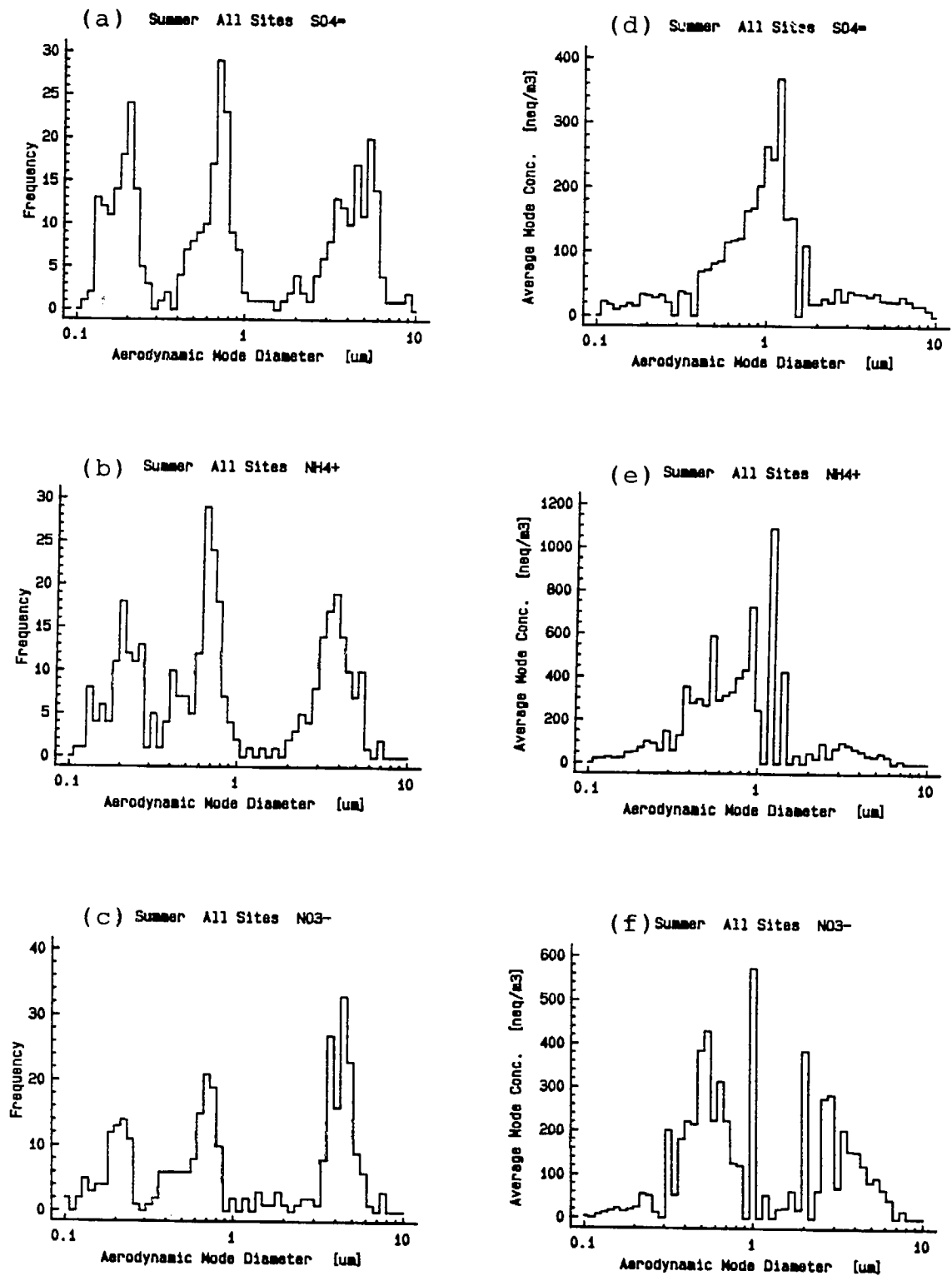


Figure 11. From all sites during summer SCAQS: Left column, frequency (no. of cases) of sulfate, ammonium and nitrate modes vs. mode diameter; right column, average sulfate, nitrate and ammonium concentration vs. mode diameter.

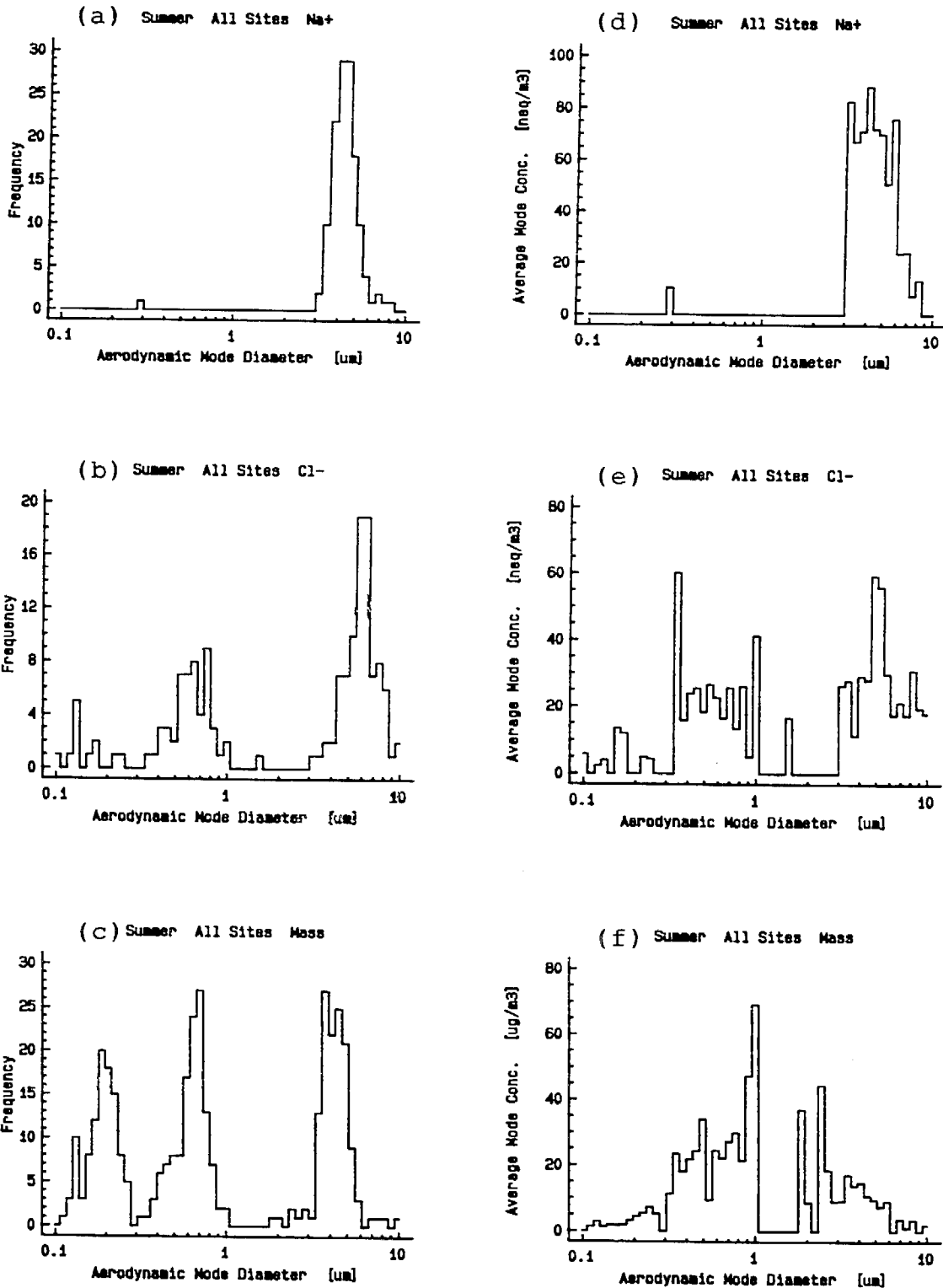


Figure 12. From all sites during summer SCAQS: Left column, frequency (no. of cases) of sodium, chloride and total ionic mass vs. mode diameter; right column, average sodium, chloride and total ionic mass concentration vs. mode diameter.

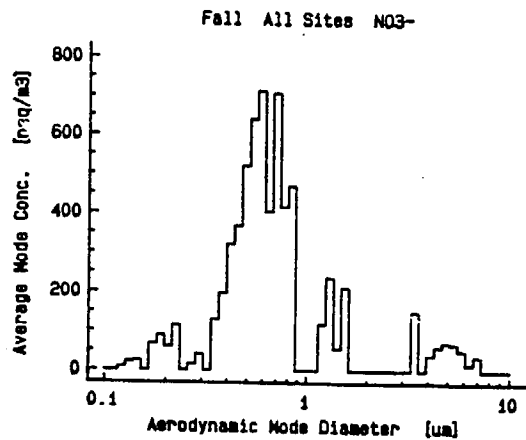
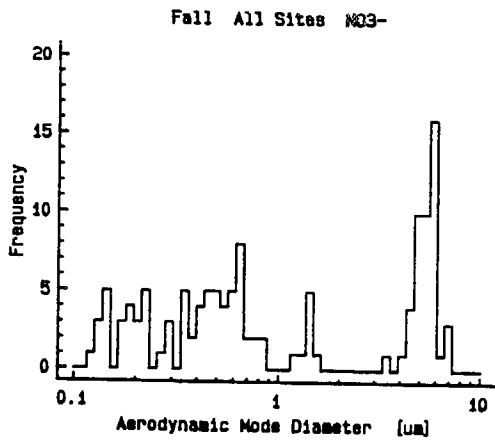
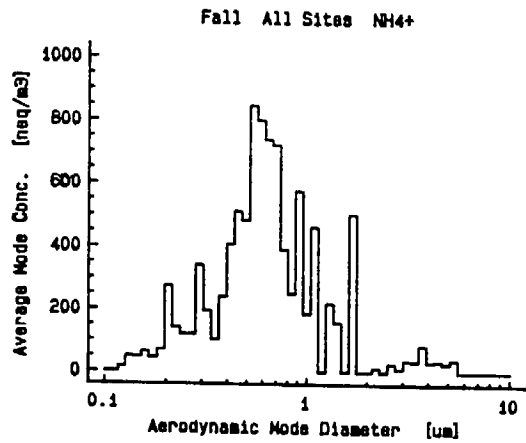
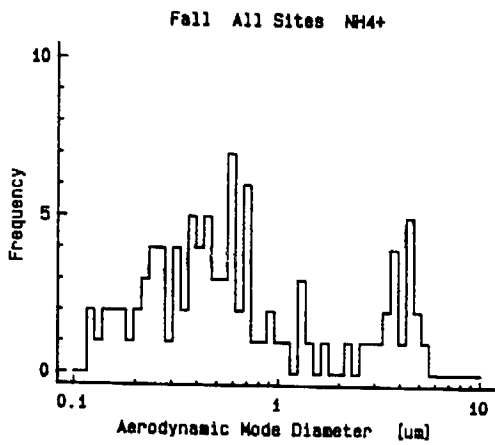
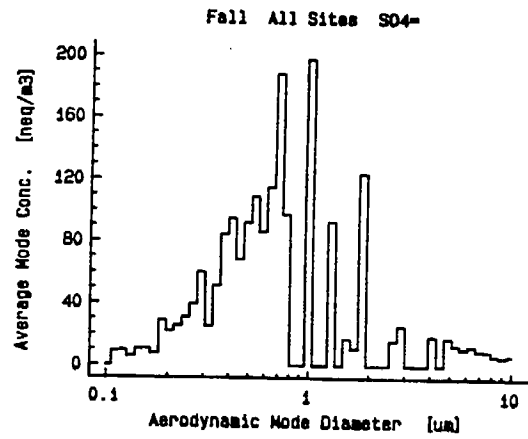
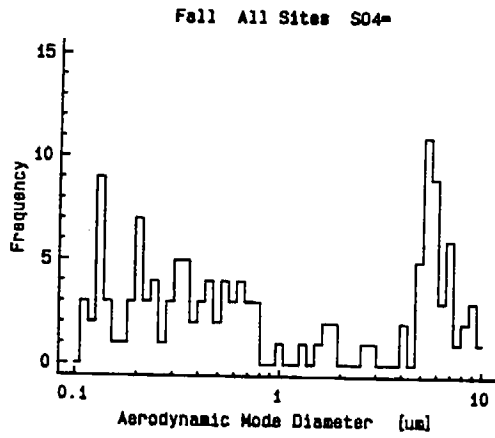


Figure 13. From all sites during fall SCAQS: Left column, frequency (no. of cases) of sulfate, ammonium and nitrate modes vs. mode diameter; right column, average sulfate, ammonium and nitrate mode concentration vs. mode diameter.

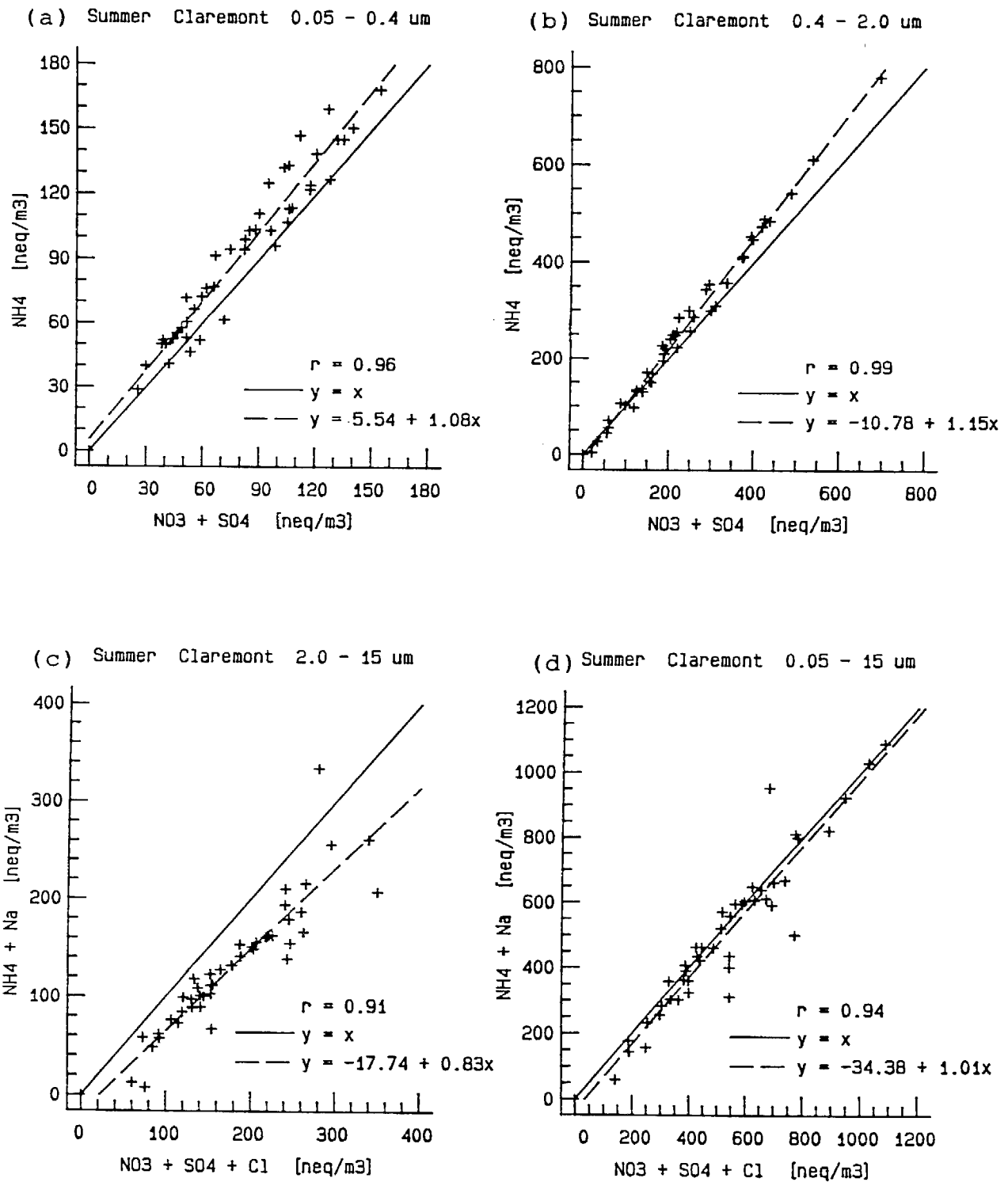


Figure 14. Ion balance plots for Claremont data during summer SCAQS for the particle size range of the (a) condensation mode, (b) droplet mode, (c) coarse mode and (d) sum of all three modes.

SUMMER N03-

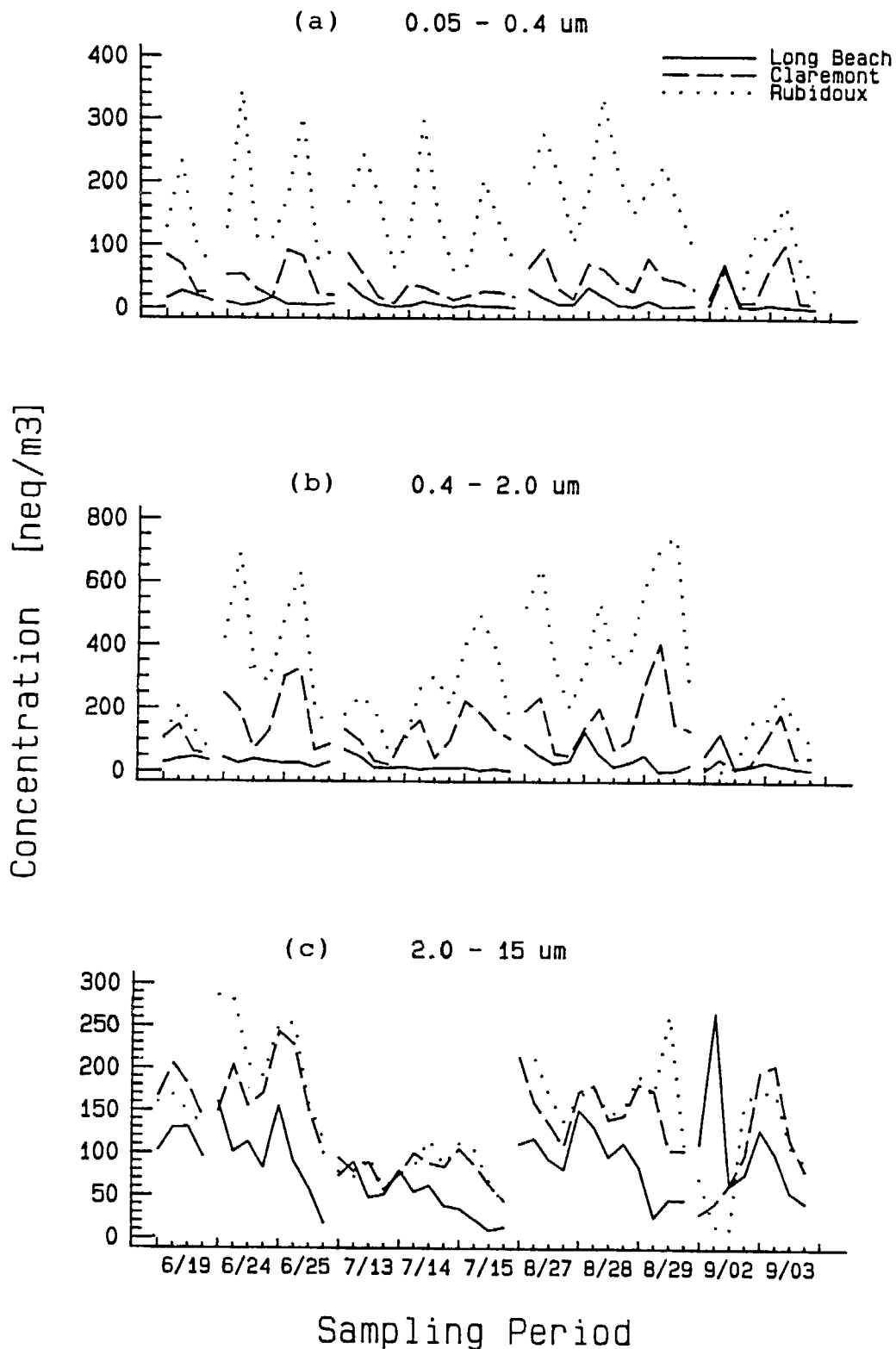


Figure 15. Time series of nitrate concentrations during summer SCAQS for the particle size range of the (a) condensation mode, (b) droplet mode and (c) coarse mode.

SUMMER SO4=

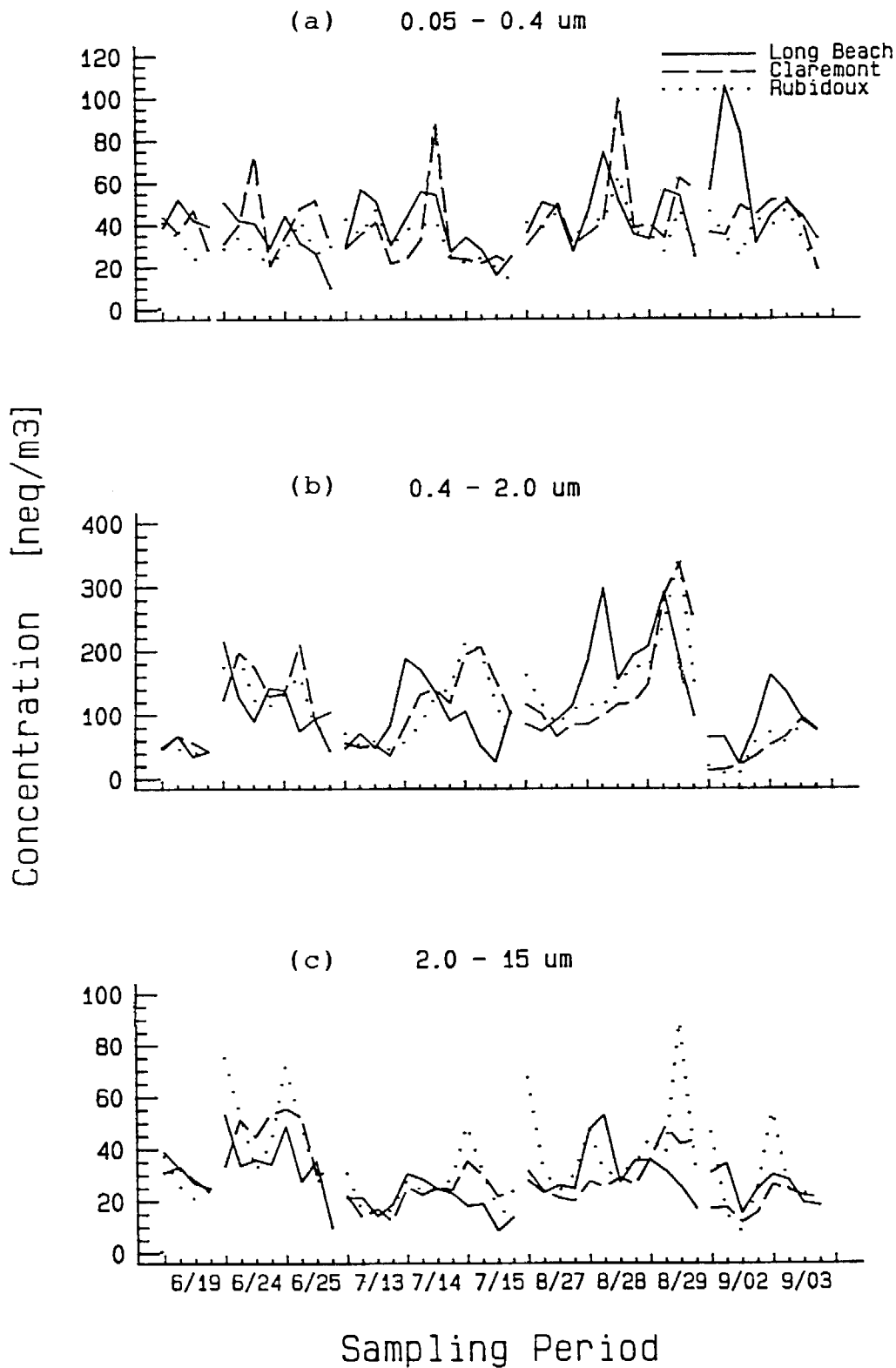


Figure 16. Time series of sulfate concentrations during summer SCAQS for the particle size range of the (a) condensation mode, (b) droplet mode and (c) coarse mode.

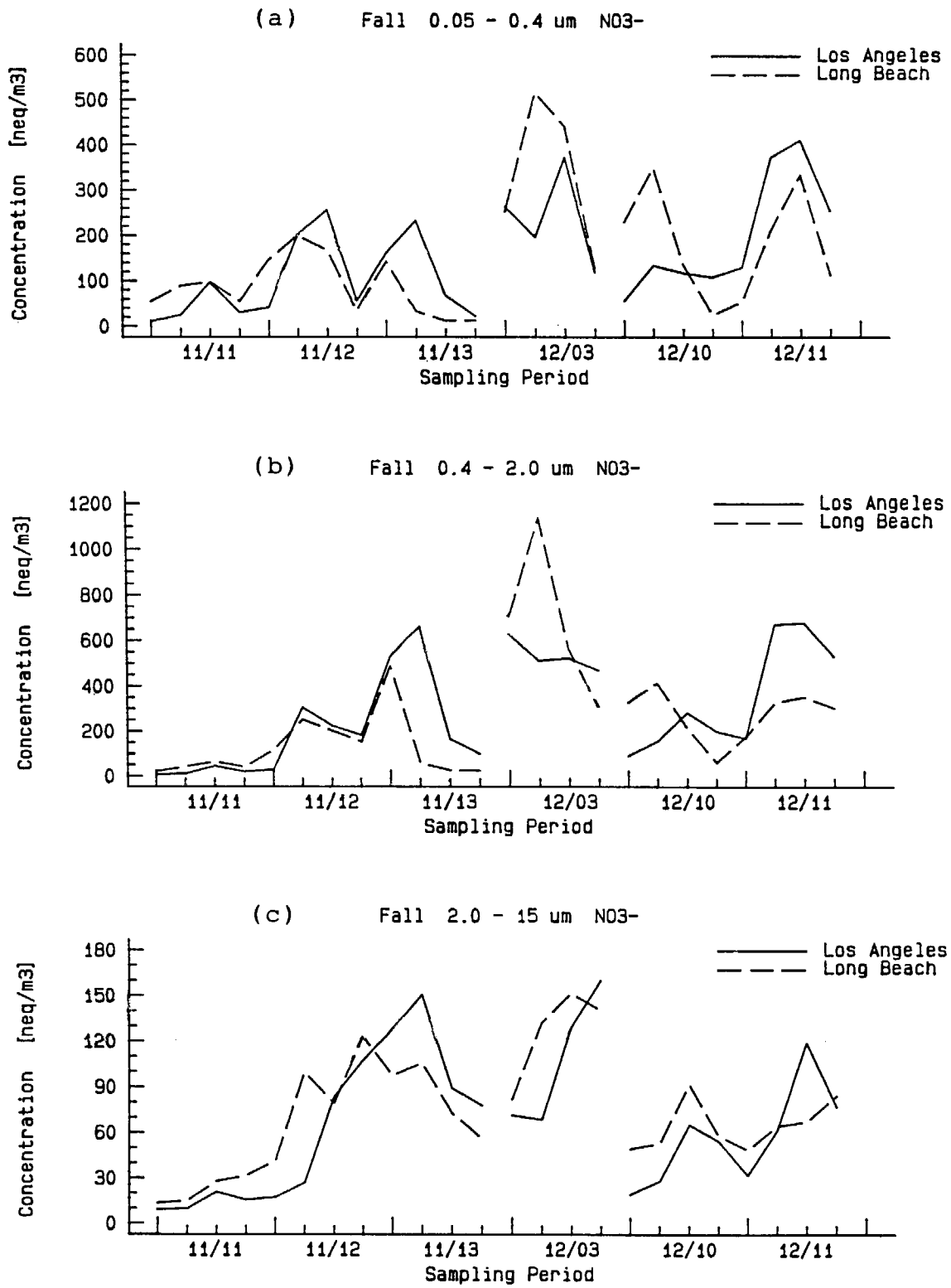


Figure 17. Time series of nitrate concentrations during fall SCAQS for the particle size range of the (a) condensation mode, (b) droplet mode and (c) coarse mode.

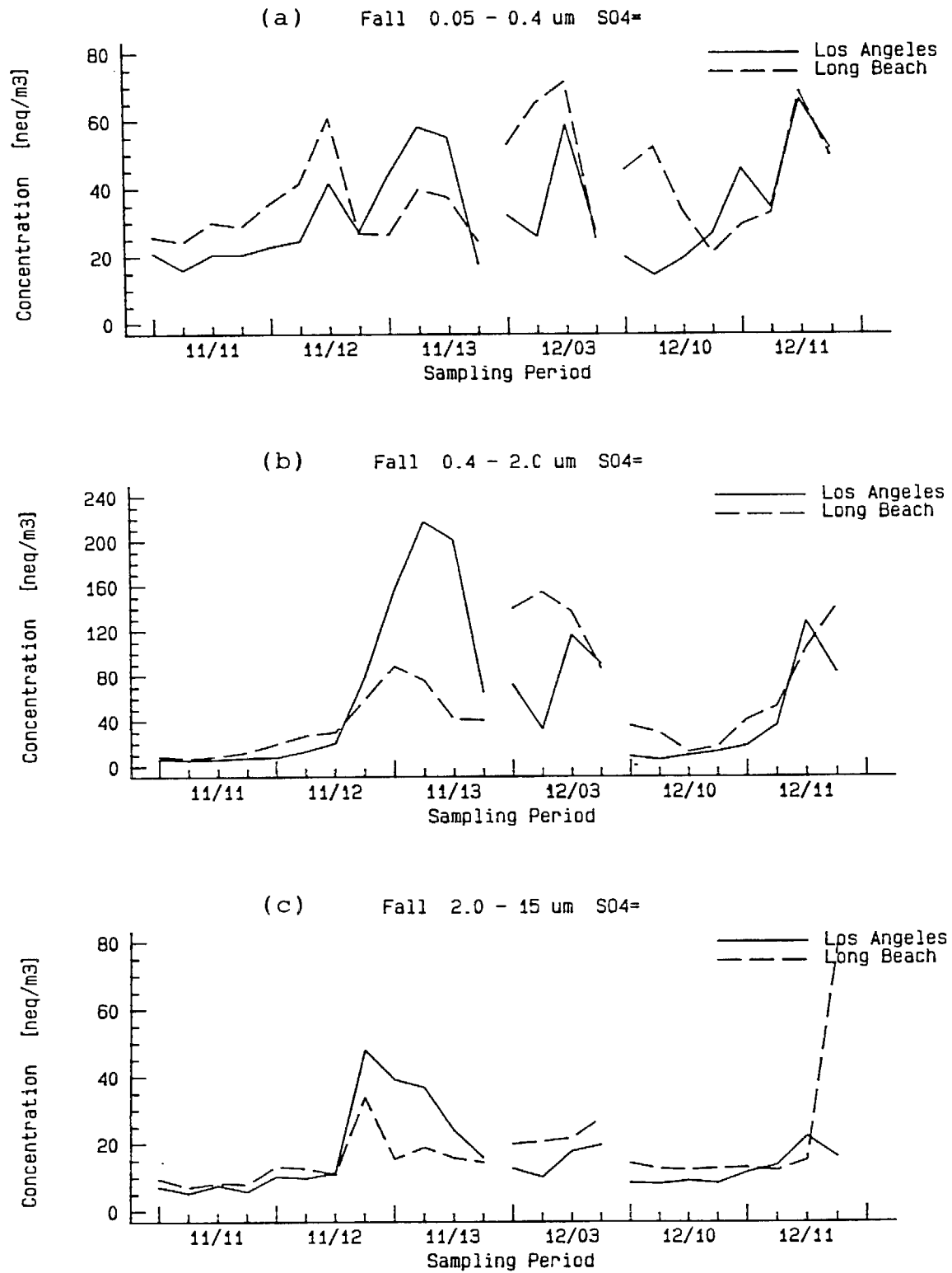


Figure 18. Time series of sulfate concentrations during fall SCAQS for the particle size range of the (a) condensation mode, (b) droplet mode and (c) coarse mode.

Claremont SO4=

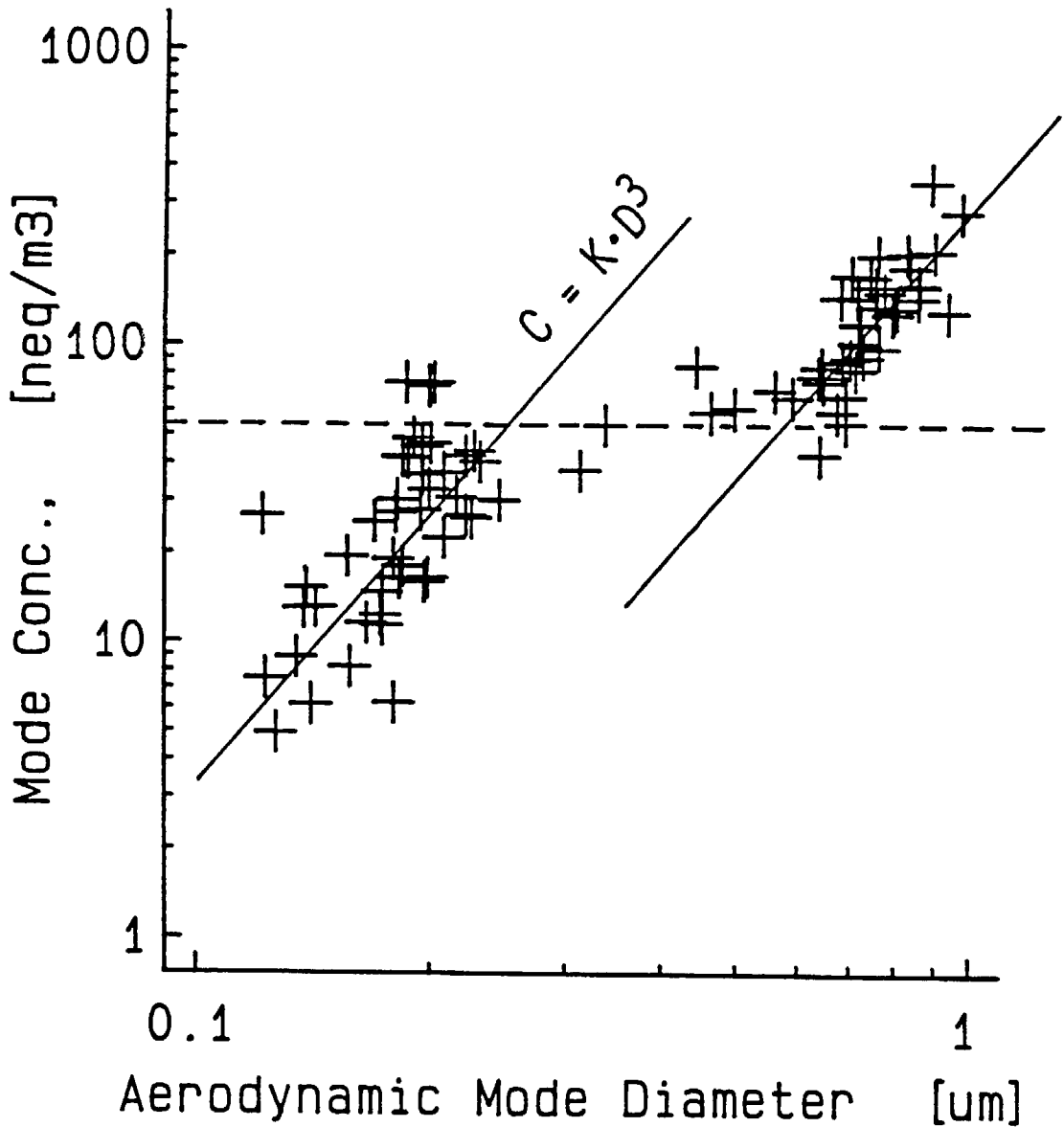


Figure 19. Log-log plot of sulfate mode concentration vs. mode diameter from Claremont during summer SCAQS. The solid lines have slopes corresponding to mode concentration increasing with the cube of the mode diameter. A transition between the two modes is believed to occur at approximately the sulfate mode concentration indicated by the horizontal dashed line.

Claremont SO4=

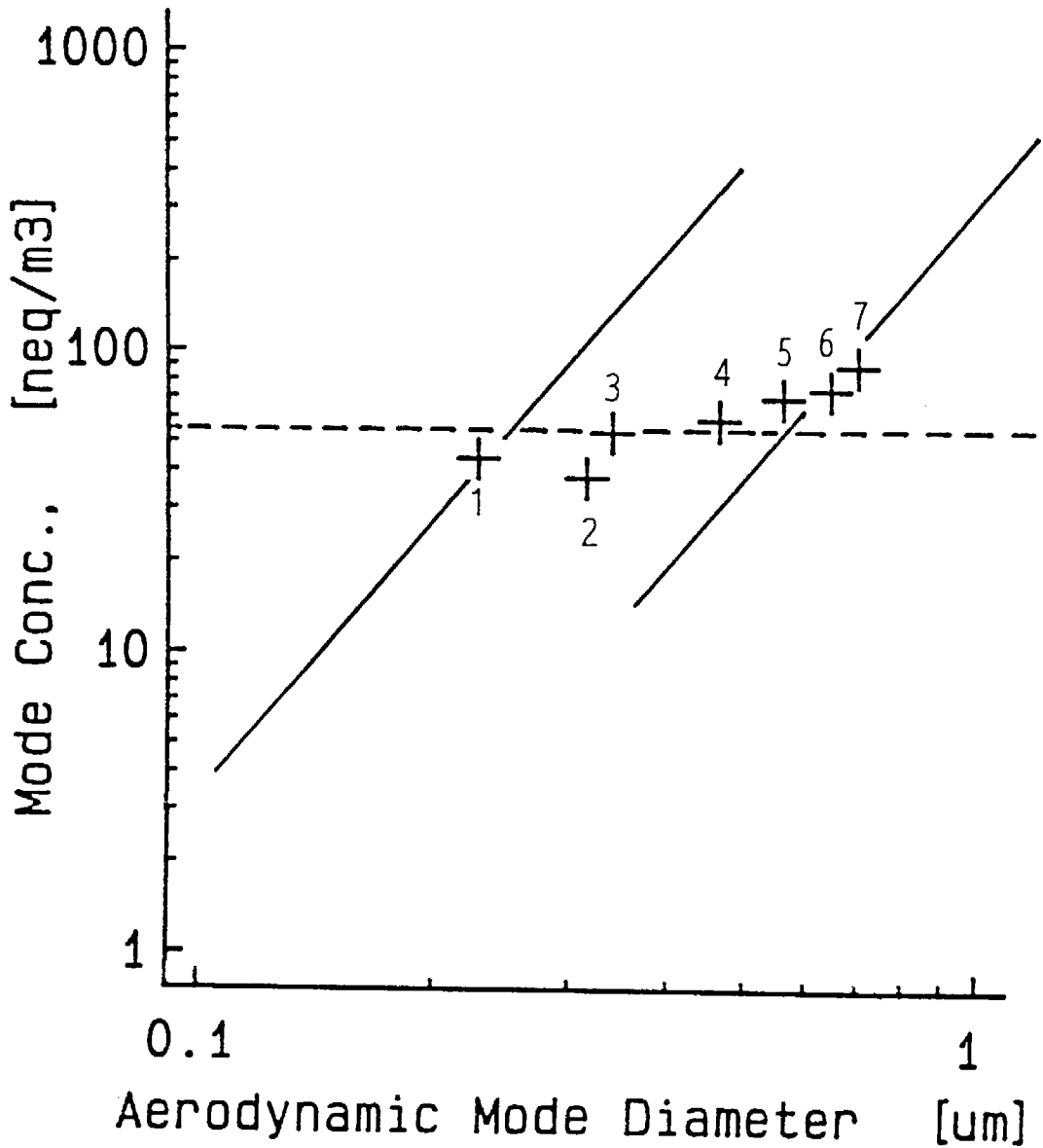


Figure 20. Plot similar to Figure 19 but the data include only the sampling periods on September 2 and the first three periods on September 3. The data points from these seven periods are in order from left to right.

00004271



ASSET

REPORT DOCUMENTATION PAGE

1. AGENCY USE ONLY (<i>Leave Blank</i>) PB90150756		2. REPORT DATE November 1989	3. REPORT TYPE AND DATES COVERED Final Report	
4. TITLE AND SUBTITLE Acidic Aerosol Size Distribution During SCAQS			5. FUNDING NUMBERS A6112-32	
6. AUTHOR(S) Walter John, Stephen M. Wall, Joseph L. Ondo and Wolfgang Winklmayr				
7. PERFORMING ORGANIZATION NAME(S) AND ADDRESS(ES) Air & Industrial Hygiene Laboratory CA Dept. of Health Services Berkeley, CA 94704-9980			8. PERFORMING ORGANIZATION REPORT NUMBER	
9. SPONSORING/MONITORING AGENCY NAME(S) AND ADDRESS(ES) California Air Resources Board Research Division 2020 L Street Sacramento, CA 95814			10. SPONSORING/MONITORING AGENCY REPORT NUMBER ARB/R-89/421	
11. SUPPLEMENTARY NOTES				
12a. DISTRIBUTION/AVAILABILITY STATEMENT Release unlimited. Available from National Technical Information Service. 5285 Port Royal Road Springfield, VA 22161			12b. DISTRIBUTION CODE	
13. ABSTRACT (<i>Maximum 200 Words</i>) Ambient aerosol in the size range 0.075-16 um was sampled with Berner Cascade impactors during the summer and fall intensive sampling periods of the Southern California Air Quality Study (SCAQS) of 1987. Deposits on the greased Tedlar stage substrates were extracted with deionized water and analyzed for inorganic anions and cations by ion chromatography. Stage mass data were converted by a modified version of the Tuomly Non-linear Herative Algorithm and modes in the converted size distributions of ionic species were obtained.				
14. SUBJECT TERMS Size distribution, accumulation mode, condensation, droplet, iognormal, impactor, inorganic, ions, sulfate, nitrate.			15. NUMBER OF PAGES 192	
			16. PRICE CODE	
17. SECURITY CLASSIFICATION OF REPORT Unclassified	18. SECURITY CLASSIFICATION OF THIS PAGE Unclassified	19. SECURITY CLASSIFICATION OF ABSTRACT Unclassified	20. LIMITATION OF ABSTRACT Unlimited	

GENERAL INSTRUCTIONS FOR COMPLETING SF 298

The Report Documentation Page (RDP) is used in announcing and cataloging reports. It is important that this information be consistent with the rest of the report, particularly the cover and title page. **Instructions for filling in each block of the form follow. It is important to stay within the lines to meet optical scanning requirements.**

Block 1. Agency use only (Leave Blank)

Block 2. Report Date. Full publication date including day, month, and year, if available (e.g. 10, Jan 88). Must cite at least the year.

Block 3. Type of Report and Dates Covered. State whether report is interim, final, etc. If applicable, enter inclusive report dates (e.g. 10 June 87 - 30 June 88).

Block 4. Title and Subtitle. A title is taken from the part of the report that provides the most meaningful and complete information. When a report is prepared in more than one volume, repeat the primary title, add volume number, and include subtitle for the specific volume. On classified documents enter the title classification in parentheses.

Funding Numbers. To include contract and grant numbers; may include program element number(s), project number(s), task number(s), and work unit number(s). Use the following labels:

C - Contract	PR - Project
G - Grant	TA - Task
PE - Program Element	WU - Work Unit Accession No.

Block 6. Author(s). Name(s) of person(s) responsible for writing the report, performing the research, or credited with the content of the report. If editor or compiler, this should follow the name(s).

Block 7. Performing Organization Name(s) and Address(es). Self-explanatory.

Block 8. Performing Organization Report Number. Enter the unique alphanumeric report number(s) assigned by the organization performing the report.

Block 9. Sponsoring/Monitoring Agency Name(s) and Address(es). Self-explanatory.

Block 10. Sponsoring/Monitoring Agency Report Number. (If known)

Block 11. Supplementary Notes. Enter information not included elsewhere such as: Prepared in cooperation with...; Trans. of...; To be published in.... When a report is revised, include a statement whether the new report supersedes or supplements the older report.

Block 12a. Distribution/Availability Statement

Denotes public availability or Limitations. Cite any availability to the public, Enter additional limitations or special markings in all capitals (e.g., NOFPRM, REL, ITAR).

DOD - See DoDD 5230.24, "Distribution Statements on Technical Documents."
DOE - See authorities.
NASA - See Handbook NHB 2200.2
NTIS - Leave blank.

Block 12b. Distribution Code.

DOD - Leave blank.
DOE - Enter DOE distribution categories from the Standard Distribution for Unclassified Scientific and Technical Reports
NASA - Leave blank.
NTIS - Leave blank.

Block 13. Abstract. Include a brief (Maximum 200 words) factual summary of the most significant information contained in the report.

Block 14. Subject Terms. Keywords or phrases identifying major subjects in the report.

Block 15. Number of Pages. Enter the total number of pages.

Block 16. Price Code. Enter appropriate price code (NTIS only).

Block 17. - 19. Security Classifications. Self-explanatory. Enter U.S. Security Classification in accordance with U.S. Security Regulations (i.e., UNCLASSIFIED). If form contains classified information, stamp classification on the top and bottom of the page.

Block 20. Limitation of Abstract. This block must be completed to assign a limitation to the abstract. Enter either UL (unlimited) or SAR (same as report). An entry in this block is necessary if the abstract is to be limited. If blank, the abstract is assumed to be unlimited.